

FORCED CONVECTION BOILING IN A COIL

By

AMOS YUDOVICH

Bachelor of Science

Technion, Israel Institute of Technology

Haifa, Israel

1959

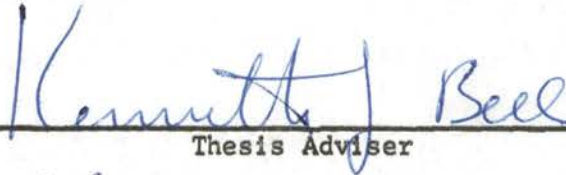
Submitted to the faculty of the Graduate School of
the Oklahoma State University
in partial fulfillment of the requirements
for the degree of
MASTER OF SCIENCE
May, 1966

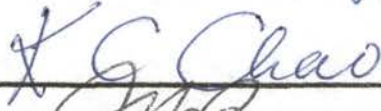
OKLAHOMA
STATE UNIVERSITY
LIBRARY

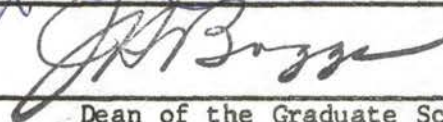
NOV 10 1966

FORCED CONVECTION BOILING IN A COIL

Thesis Approved:


Thesis Adviser





Dean of the Graduate School

621882

PREFACE

This work contains an investigation of boiling of n-hexane and water in a coil.

The flow of liquid inside a coil under boiling conditions was explored and tested. Design details and results of the experimental runs are presented in this thesis.

An additional variable--the radial acceleration--was introduced to explain some of the phenomena of boiling in this system.

It has become almost a tradition that any work dealing with the subject of boiling heat transfer should start by recognizing the complexity of the phenomenon. This complexity is especially what makes boiling heat transfer so challenging. I am deeply indebted to Dr. Kenneth J. Bell who helped me so much to face this challenge, by his most useful advice, encouragement and inspiration. I am also grateful to the members of the thesis committee Dr. J. H. Erbar and Dr. J. W. Fulton for their helpful remarks and aid.

I wish to express my gratitude to Black, Sivalls & Bryson Inc., which supplied the boiler shell for this experiment.

I am also indebted to the School of Chemical Engineering, Oklahoma State University which granted me financial support during the course of this work.

TABLE OF CONTENTS

Chapter	Page
I. INTRODUCTION.	1
II. FUNDAMENTALS OF BOILING	3
Boiling Regions.	3
Burnout.	4
III. SURVEY OF LITERATURE.	6
Boiling and Boiling Mechanisms	6
Boiling and Gravity Fields	8
IV. THEORETICAL ANALYSIS OF BOILING IN A COIL	11
The Effect of Radial Acceleration on Boiling Inside a Tube	12
Heat Transfer Mechanism in a Coil.	16
Boiling Heat Flux Determination.	19
Experimental Testing of the Theoretical Model.	20
V. EXPERIMENTAL APPARATUS.	21
Auxiliary Equipment	22
VI. EXPERIMENTAL PROCEDURE.	29
Start-Up Procedure	29
Measurement and Data Recording Procedure	30
VII. EXPERIMENTAL RESULTS AND CORRELATED DATA.	32
Experimental Results	32
Correlation of Data.	33
Experimental Errors.	33
VIII. DISCUSSION OF RESULTS, CONCLUSIONS AND RECOMMENDATIONS.	44
Recommendations.	46
BIBLIOGRAPHY	47
APPENDIX A - EXPERIMENTAL AND CALCULATED DATA.	49

APPENDIX B - SAMPLE CALCULATIONS 70
 Estimation of Boiling Heat Flux 71
 Dimensionless Radial Acceleration 73
APPENDIX C - THERMOCOUPLE CALIBRATION PROCEDURE. 74
 Calibration of the Reference Thermocouple 75
APPENDIX D - ROTAMETER AND ORIFICE CALIBRATION 79
NOMENCLATURE 86

LIST OF TABLES

Table	Page
I. Flow Rates and Temperatures Data for n-Hexane.	50
II. Flow Rates and Temperatures Data for Water	51
III. Heat Balance Data for n-Hexane	52
IV. Heat Balance Data for Water.	53
V. Heat Transfer Data--n-Hexane	54
VI. Heat Transfer Data--Water.	55
VII. Radial Acceleration and Boiling Heat Fluxes for n-Hexane . .	56
VIII. Radial Acceleration and Boiling Heat Fluxes for Water at Partial Evaporization.	57
IX. Radial Acceleration and Boiling Heat Fluxes for Water at Total Evaporization.	57
X. Pressures at Boiler Inlet.	58
XI. Thermocouple Reading Along the Coil.	59
XII. Temperature Distribution Along the Coil.	63
XIII. Calibration of the Reference Thermocouple.	75
XIV. Thermocouple Reading Correction--Low Temperature	77
XV. Thermocouple Reading Correction--High Temperature	78
XVI. Cooling Water Orifice Flow Meter Calibration	80
XVII. Rotameter Calibration for n-Hexane	82
XVIII. Rotameter Calibration for Water.	84

LIST OF FIGURES

Figure	Page
1. Boiling Curve	3
2. Radial Acceleration in Flow in a Coil	13
3. Regimes of Flow and Heat Transfer in a Vertical Tube.	14
4. Flow and Heat Transfer Model for a Coil	15
5. Temperature Difference in a Cross Section of the Tubing	18
6. Flow Sheet Diagram.	23
7. The Coil and the Thermocouple Connections	24
8. General View of Apparatus and Auxiliary Equipment	25
9. Boiler Shell, Steam Demister and Flow Meters.	25
10. Instrument Panel.	26
11. Boiler Shell Insulation and Thermocouple Wiring	26
12. Piping.	27
13. Boiling Fluid Tank and Vapor Condenser.	27
14. Temperature Difference Between Steam and Outlet Stream for n-Hexane.	34
15. Temperature Difference Between Steam and Outlet Stream for Water	35
16. Boiling Heat Flux of n-Hexane vs. Flow Rate	36
17. Boiling Heat Flux of Water vs. Flow Rate.	37
18. Temperature Profile Along the Coil.	38
19. Dimensionless Radial Acceleration vs. Per Cent of Vapor for n-Hexane and Water.	39
20. Boiling Heat Flux of n-Hexane vs. Dimensionless Radial Acceleration.	40

21.	Boiling Heat Flux of Water vs. Dimensionless Radial Acceleration.	41
22.	Boiler Inlet Pressure vs. Flow Rate of n-Hexane	42
23.	Boiler Inlet Pressure vs. Flow Rate of Water.	42
24.	Cooling Water Orifice Calibration Curve	81
25.	Rotameter Calibration Curve for n-Hexane.	83
26.	Rotameter Calibration Curve for Water	86

CHAPTER I

INTRODUCTION

Heat transfer to fluids in a condition involving more than one fluid phase is probably of greater industrial significance than any other heat transfer process. Boiling heat transfer is widely employed in high performance systems owing to the fact that extremely high heat transfer fluxes may be obtained with relatively low surface to fluid temperature differences.

The effect of high gravitational fields on boiling has some technical importance where boiling occurs in a rapidly accelerating system. Modern high-performance devices such as rockets and missiles in the initial stages of flight or a space craft during its re-entry to earth are examples of such systems. With various new problems encountered in space technology it may be expected that boiling will occur in force fields other than that of earth.

Little information has been published on the influence of gravitational and other acceleration forces on boiling. In the few papers published recently on this subject the researchers are not in much agreement as far as the influence of gravitation on boiling is concerned (6, 7, 8, 19, 28, 33, 34, 35).

The main purpose of the present work was to gain some insight into the mechanism of boiling in a coil, in which the fluid experiences radial acceleration.

The following goals were set for this project:

- (1) Design an apparatus which may be used to study the boiling of n-hexane and water in a coil using low pressure steam as the heating medium.
- (2) Using the apparatus, obtain information on boiling of n-hexane and water such as exit vapor fractions, surface temperature distribution and heat loads at various liquid inlet velocities.
- (3) Analyze and correlate these data.

CHAPTER II

FUNDAMENTALS OF BOILING

Boiling Regions

When a liquid at its saturation temperature T_{sat} , at a given pressure is boiling on an heater surface at temperature T_w which supplies q/A BTU per hour per square foot, and the heat flux is varied, it is observed that the temperature difference between the heater surface and the saturated liquid varies also. When the heat flux is plotted versus the temperature difference the following boiling curve will be obtained:

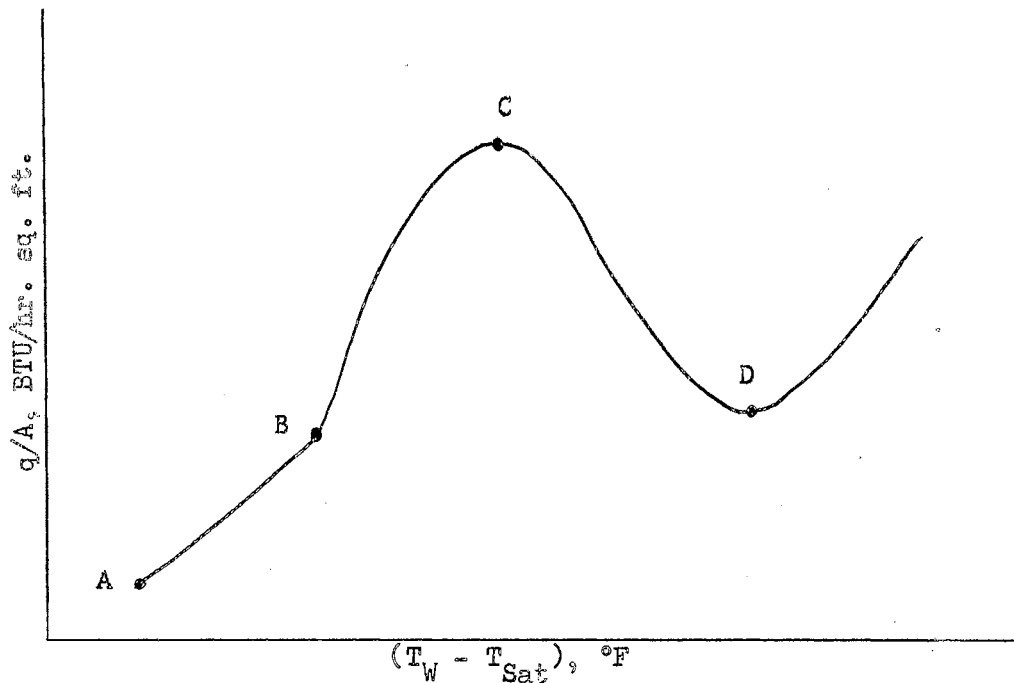


Figure 1. Boiling Curve

In the region AB in Figure 1 the heat is transferred by conduction through the liquid and natural convection currents.

The region BC in Figure 1 is nucleate boiling. Here bubbles form at specific preferred points on the hot surface, called active nucleation sites.

The boiling so improves the efficiency of the heat transfer process that the amount of heat transferred now rises rapidly with only a small further increase of surface temperature.

As the surface temperature is increased still further however, a point is reached (at point C Figure 1) where the heat flux reaches a maximum. The heat flux at which this condition occurs is called the "peak heat flux." The temperature difference at point C is called the "critical temperature difference." In this region the bubbles begin to coalesce to give a partial vapor blanketing. In the partial vapor blanketing region, (region CD in Figure 1) the heat transfer is poor since the vapor is a poor heat conductor. The vapor blanketing becomes complete at point D Figure 1. The region CD Figure 1 is commonly termed the transition region. From point D in Figure 1 on beyond indefinitely to increasing temperature differences, film boiling exists. In film boiling a layer of vapor coats the hot surface and the heat is transferred through the film by conduction and radiation.

Burnout

Nucleate boiling from a solid surface takes place within a certain temperature difference range only. As the temperature-difference increases, the heat transfer increases, up to a point (point C in Figure 1). This point is called the burnout point. The existence of an upper limit

to nucleate boiling is of extreme importance to engineers. If for a short time the heat supplied to the heater exceeds the heat transferred to the boiling liquid, heat would accumulate in the heater surface and its temperature would rise. The heat source plays a dominant role in the burnout phenomenon, i.e. the result of exceeding the critical temperature difference. If the heat is supplied from a condensing vapor or from a hot fluid, the unsteady state is self-regulating. Any decrease in h_B causes an increase in the wall temperature and a decrease in the driving force from the solid surface to the boiling fluid. The heat flux decreases and a new steady state is established. This results in a more or less smooth operation in the transition region of boiling. The heat transfer surface will not be overheated and destroyed, but the operation conditions will be inefficient.

If the heat is generated by chemical, nuclear or electrical sources in which the heat flux is fixed, the results are entirely different. The unsteady-state condition resulting from slightly exceeding the critical temperature difference is not self controlled. If h_B decreases, the surface temperature will increase, but this will have no effect on the heat flux. Heat will accumulate in the surface until it melts or until the value of $h_B \Delta T$ increases sufficiently to equal the heat flux and re-establish a new steady state in the film boiling regime.

CHAPTER III

SURVEY OF LITERATURE

Boiling and Boiling Mechanisms

A survey of the literature reveals that the first information on boiling was published by Leidenfrost in 1756 (10, 23). Lang in 1888 (22) had been aware of the existence of minimum and maximum heat flux rates in boiling. But the existence of several regimes of boiling was first clearly discussed by Nukiyama (29).

Photography, especially with high speed cameras, has contributed substantially to a better understanding of boiling mechanism (5, 10, 20, 36).

Bonilla and Perry (1), Cryder and Finalborgo (9), Insinger and Bliss (18) and others developed empirical correlations for nucleate boiling. These correlations were derived basically from dimensional analysis. The various authors are in no agreement on the relative importance of variables involved in boiling such as viscosity, density, surface tension and temperature differences. The above mentioned correlations have met with poor success.

Nucleate boiling, which is the most common type of boiling, has received much more attention in the literature compared to the other types of boiling.

The two prevailing approaches to the mechanism of nucleate boiling are those of Rohsenow and co-workers (30, 31, 32) and Forster, Zuber

and co-workers (11, 12, 13, 14, 37).

Both approaches are theoretical in part and empirical in part. Both assume that during nucleate boiling heat flows from the hot solid surface into the liquid and from thence to vapor bubbles.

According to Rohenow (30) the controlling step in nucleate boiling is the movement of bubbles at the instant of breaking away from the hot surface. This movement of bubbles is presumed to give agitation, improving convection currents and consequently increasing the heat transfer coefficient.

Forster and Zuber on the other hand have postulated that the size of the bubbles at the instant of their departure is of prime importance and the movement of the bubbles up into the bulk of liquid has little influence on the rate of heat transfer.

Forster and Greif (14) suggested that the bubbles act in a mechanical manner to pump superheated liquid into the colder region, and the heat transferred by each bubble q_b is given by the following proportionality:

$$q_b \propto C_L \rho_L R_{\max}^3 f \Delta T \quad (1)$$

(in which f is the bubble departure frequency). Jakob (21) observed the frequency of bubble formation in nucleate boiling of a pool of water and found that the time was in the order of 0.05 sec.

McFadden and Grassman (25) studied the relation between the bubble frequency and diameter during boiling of liquid nitrogen and found experimentally that the frequency of bubble departure from its site can be expressed by the following relationship:

$$f D^{\frac{1}{2}} \propto 0.56 g^{\frac{1}{2}} \quad (2)$$

By a force balance on the departing bubble the following relation was obtained:

$$f D^{\frac{1}{2}} = \text{constant} \quad (3)$$

which agreed with the experimental results.

Two useful correlations for the nucleate boiling regime were given by Zuber (37) and by McNelly (26).

Numerous studies have been made recently on the peak heat flux due to the great development in nuclear technology (5, 16, 17).

Film boiling has received less attention in the literature than nucleate boiling. It is characterized by its slower action and better defined compared to nucleate boiling. Film boiling is the first type of boiling to be attacked, with success, from a theoretical standpoint. Boiling heat transfer in most of the film region is described fairly well by the equations of Bromley (2, 3). Bromley derived a semi-theoretical equation for film boiling assuming laminar flow of vapor and heat transfer by conduction through the film.

An experiment by Westwater (36) using a high speed motion picture camera showed that during film boiling no active centers exist and no vapor was generated on the solid surface, but all bubbles were generated at the liquid-vapor interface.

Boiling and Gravity Fields

The study of the influence of a force field on boiling has been receiving some attention in the last few years and reports on that subject are found recently in the literature.

Costello and Adams (8) ran a pool boiling test wherein the pool was rotated to produce radial accelerations normal to a flat surface up to 40 g. Their data for peak heat flux showed:

$$(q/A)_p \propto (a/g)^{0.15} \quad (4)$$

for $a/g \leq 10$ and,

$$(q/A)_p \propto (a/g)^{0.25} \quad (5)$$

for $a/g > 10$. Equation (5) is in fair agreement with the proposed burnout prediction equations suggested by Zuber (37).

Ivey (19) conducted similar tests using a high speed centrifuge and found that equation (4) held over the range $1 \leq a/g \leq 160$.

Costello and Tuthill (7) tested the effect of acceleration on nucleate boiling under similar conditions, using heat fluxes from 100,000 BTU/hr-sq ft to 200,000 BTU/hr-sq ft and acceleration from 1 g up to 40 g. They observed an increase in ΔT with acceleration. These researchers concluded that the boiling heat transfer coefficient is adversely affected by acceleration.

Pool boiling experiments in accelerating systems have been conducted also by Merte and Clark (28), using a centrifuge to produce acceleration up to 20 g. In this work temperature differences have been measured at various heat fluxes. Merte and Clark reported that the influence of acceleration was greatest at heat fluxes up to 50,000 BTU/hr-sq ft; within this range, acceleration decreased the ΔT . But with higher heat fluxes, from 50,000 BTU/hr-sq ft to 200,000 BTU/hr-sq ft a reversal of the effect of acceleration was observed, i.e. ΔT increased with acceleration, which was in agreement with the experiments of Costello and Tuthill (7).

An experimental study of boiling in reduced and zero gravity fields have been conducted by Usiskin and Siegel (35). The effect of reduced gravity on nucleate boiling bubble dynamics in water has been studied by Siegel and Keshock (34); in these studies it was observed that the burnout heat flux decreased with decrease in gravity. The existence of steady-state was uncertain in the experiments of Usiskin and Siegel and their

conclusions should be regarded as possibly questionable.

A photographic study of boiling in absence of gravity has been conducted by Siegel and Usiskin (33) and indicated that gravity field played a very important role in the removal of vapor from the surface.

Gambill and Greene (15) studied heat transfer and boiling burnout with subcooled water in vortex flow, where high values of acceleration were induced owing to the vortex motion of water. They found a marked improvement in heat transfer behaviour and a great increase in peak heat flux with acceleration according to:

$$(q/A)_p \propto (a/g)^{0.43 - 0.48} \quad (6)$$

In Gambill and Greene's experiment the water was below its saturation temperature. Also, extremely large effects of forced circulation were superimposed upon the boiling and the increase in $(q/A)_p$ cannot be positively ascribed to acceleration effects only.

CHAPTER IV

THEORETICAL ANALYSIS OF BOILING IN A COIL

In this chapter the analysis of boiling inside a coil will be discussed. A theoretical model will be suggested introducing the effect of radial acceleration on boiling. The discussion will be confined to the case of condensing steam outside the coil.

The following assumptions were made in this work:

- (1) Steady-state conditions exist.
- (2) One-dimensional flow in the direction perpendicular to the radius of the coil.
- (3) The volume occupied by the liquid is negligible compared to that of the vapor.
- (4) The vapor and the liquid flow at the same linear velocity.

A qualitative picture of the boiling in a coil can be obtained by introducing a new variable, the radial acceleration acting perpendicular to the surface and toward the center of the coil. Because of the substantial difference between the densities of the liquid and the vapor (at moderate pressures), the acceleration acting on the boiling fluid might influence the flow and heat transfer pattern, as postulated in the following. The radial acceleration induced by the fluid will establish radial transport of liquid in the direction of the radius vector of the coil and of vapor in the opposite direction.

The radial acceleration is given by:

$$a_r = U^2/R \quad (7)$$

where U is the local linear velocity of the boiling fluid, or the tangential velocity, and is given by:

$$U = (\rho_L/\rho_V) U_o x \quad (8)$$

if the liquid and vapor are at the same velocity. The dimensionless radial acceleration is a_r/g . Thus,

$$\frac{a_r}{g} = \frac{(\rho_L/\rho_V) U_o x^2}{R g} \quad (9)$$

For an experiment with small pressure differences (ρ_L/ρ_V) can be taken as constant, and equation (9) can be written in the following form,

$$a_r/g = C U_o^2 x^2 \quad (10)$$

and for a given inlet velocity U_o ,

$$a_r/g = C' x^2 \quad (11)$$

Equation (11) shows that for a given flow rate the acceleration is a function of the vapor fraction (or quality) x . The vapor fraction x increases continuously with the distance along the coil tubing, thus a_r/g is a minimum at the beginning of the boiling section ($x = 0$), and a maximum at the beginning of the vapor superheating section ($x = 1.0$). In this section the change in a_r/g is negligible compared to that of the boiling section and depends upon the change in the superheated-vapor density.

Figure 2 shows the direction of the radial acceleration and the position of the liquid and vapor inside the coil.

The Effect of Radial Acceleration on Boiling Inside a Tube

Boiling heat transfer to a fluid flowing inside a tube, is affected by the various flow parameters and the quality, as well as by the parameters which are pertinent in pool boiling.

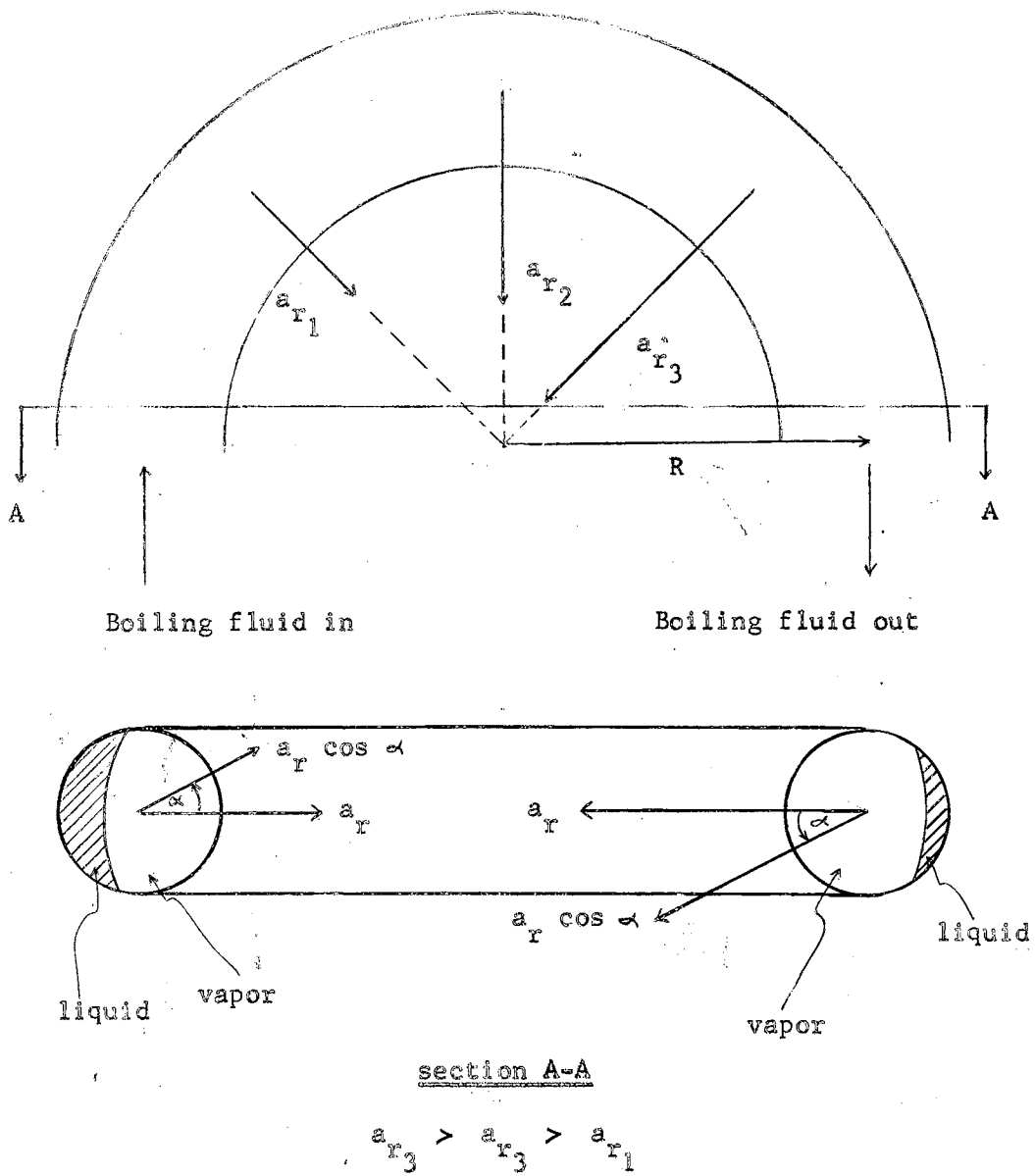


Figure 2. Radial Acceleration in Flow in a Coil

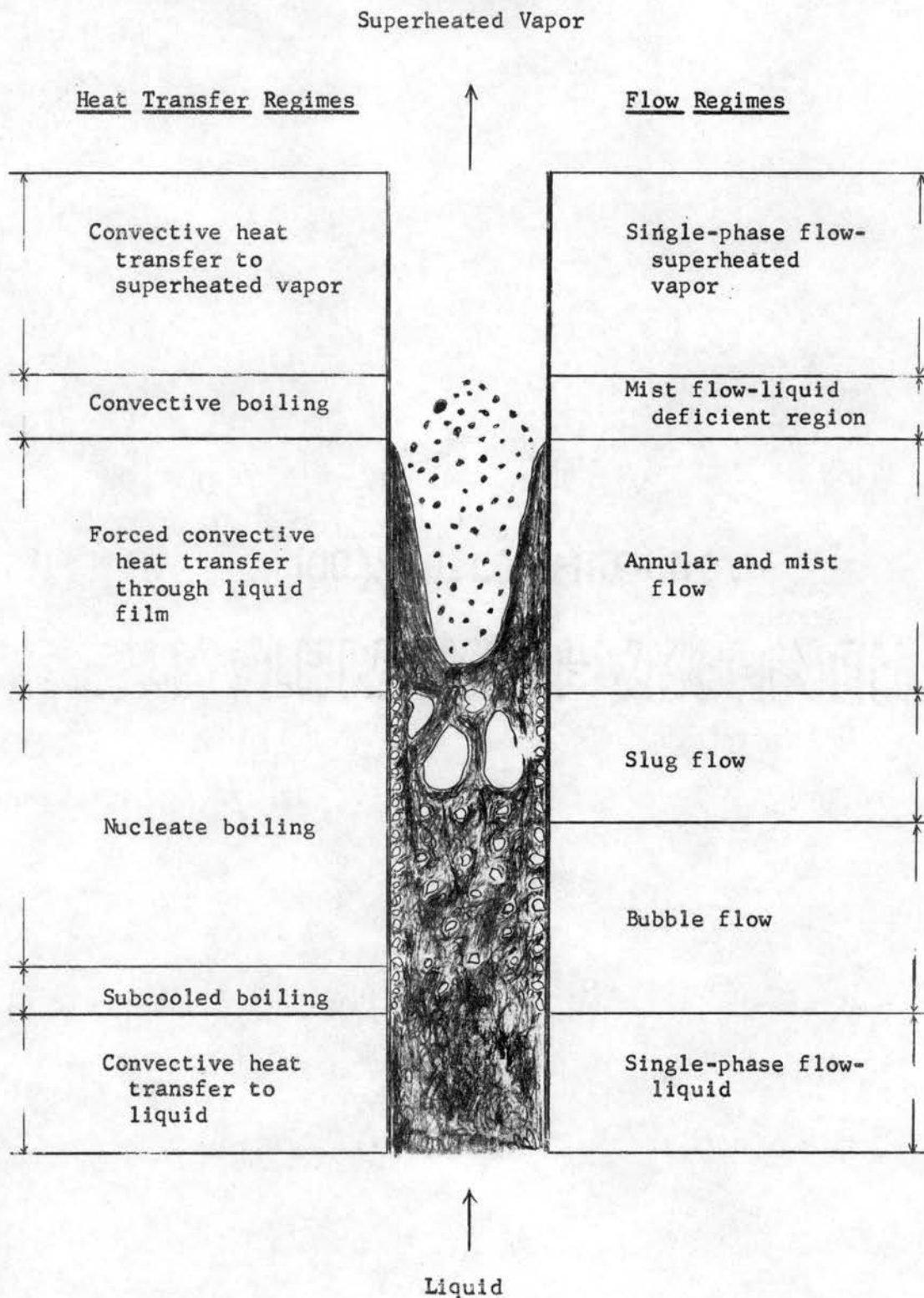
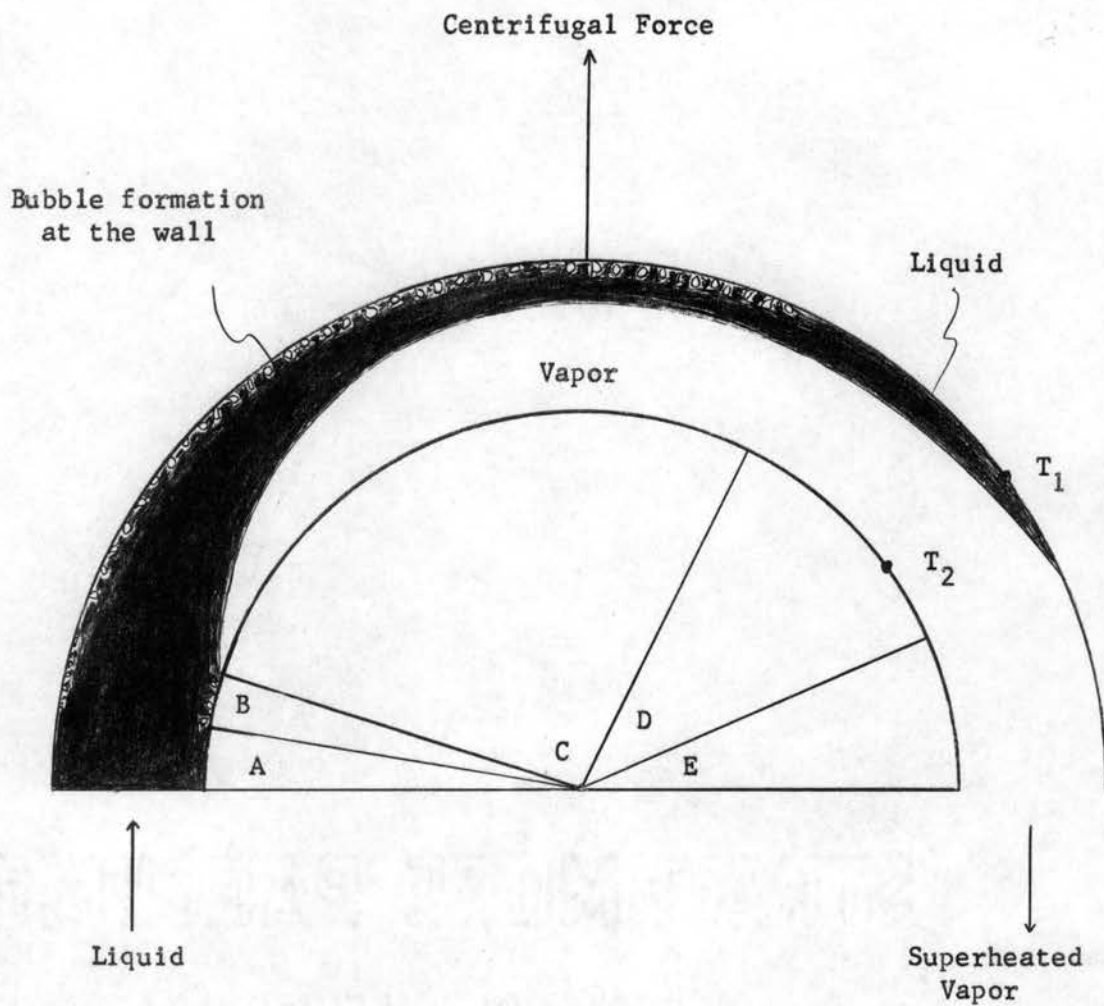


Figure 3. Regimes of Flow and Heat Transfer in a Vertical Tube



<u>Region</u>	<u>Heat Transfer</u>	<u>Fluid Flow</u>
A	Convection to liquid	Single phase-liquid
B	Subcooled boiling	Single phase-liquid
C	Nucleate boiling	Two separate phase flow
D	Convection through liquid and superheated vapor	Two separate phase flow
E	Convection to superheated vapor	Single phase-superheated vapor

Figure 4. Flow and Heat Transfer Model for a Coil

Figure 3 illustrates the wide range of local conditions and different flow regimes which could exist along the length of a vertical tube. Figure 4 shows an idealized boiling situation in a coil.

In Figure 3 and Figure 4 are shown the differences in flow pattern and heat transfer mechanism between a liquid boiling in a straight tube and in a coil. The slug flow, annular flow and mist flow regimes presumably do not exist in the coil due to the radial acceleration.

Heat Transfer Mechanism in a Coil

In the single phase flow sections there is no difference between the flow mechanism in a coil and that of a straight tube.

As the liquid proceeds up the coil, subcooled nucleate boiling starts, and vapor bubbles form on the wall and condense in the liquid. In a straight tube, the vapor bubbles will collapse and condense very close to the heated surface, thus transferring their latent heat mainly to the liquid layer near the surface. In a coil, it is assumed that the bubbles will be driven far away from the surface into the bulk of the liquid before condensing and thereby increase the transport of heat in the fluid.

In the nucleate boiling region in a straight tube, vapor bubbles are formed on the wall; some of them cling to the wall and some coalesce to form slugs. As the amount of vapor increases, the velocity of the liquid-vapor mixture increases. In the coil on the other hand, the radial acceleration increases the buoyant forces acting on the vapor bubbles in the direction toward the center of the coil. Consequently the contact time of the bubbles with the wall will be shortened and their critical diameter (i.e. the bubble diameter at its departure) will be

smaller. The bubbles will move in the direction of the radial acceleration as they detach from the surface, and two separate continuous phases will be formed. The radial acceleration increases continuously with increasing vapor fraction. The heat transfer area between the hot surface and the fluid increases for vapor and decreases for liquid.

It is postulated that there are two basic mechanisms which take part in heat transfer for boiling of liquids with flow. These are (1) the ordinary macroconvective mechanism of heat transfer, and (2) the microconvective mechanism associated with bubble nucleation and growth. It is further postulated that the radial acceleration affects the macroconvection part by the de-entrainment of the dispersed liquid in the vapor phase and the various flow characteristics, and the microconvection part due to the change in vapor bubble contact time, departure velocity and critical diameter. It is also assumed that the heat fluxes associated with those two mechanisms are additive in their contribution to the total boiling heat flux. The boiling heat flux is therefore obtained as the sum,

$$(q/A)_B = (q/A)_{mac} + (q/A)_{mic} \quad (12)$$

A change in the flow pattern, such as change in fluid velocity, or de-entrainment of the liquid particles from the vapor phase, will affect the macroconvection heat flux and consequently the total boiling heat flux. Similarly, a change in the boiling characteristics such as a change in the hot surface texture, surface tension of the liquid, vapor bubble size and velocity at departure from the hot surface, and vapor bubble frequency will affect the microconvection heat flux and consequently the total boiling heat flux. The boiling of a liquid flowing inside a tube at the annular part is an example of boiling due to macroconvection heat transfer

only. Pool boiling on the other hand, is an example of boiling due to microconvection heat transfer only. Boiling heat transfer in the nucleate boiling portion for a liquid flowing inside a heated tube is an example of a combination of macro- and microconvection boiling.

At low quality the de-entrainment effect and its influence on the macroconvective part is smaller than at high quality. Whether $(q/A)_{mic}$ would increase or decrease due to the radial acceleration imposed on the boiling liquid is to be determined.

At high quality, the de-entrainment is of great advantage. In the mist flow region and the upper part of the plug flow (see Figure 3) the vapor blankets the wall almost completely, and consequently the heat transfer is poor. The centrifugal force will push the dispersed liquid particles to the hot surface improving the heat transfer.

Since two separate phase flow is foreseen the wall temperature on the vapor side is therefore expected to be higher than that on the liquid side, referring to Figure 4. $T_2 > T_1$ and the vapor close to the wall

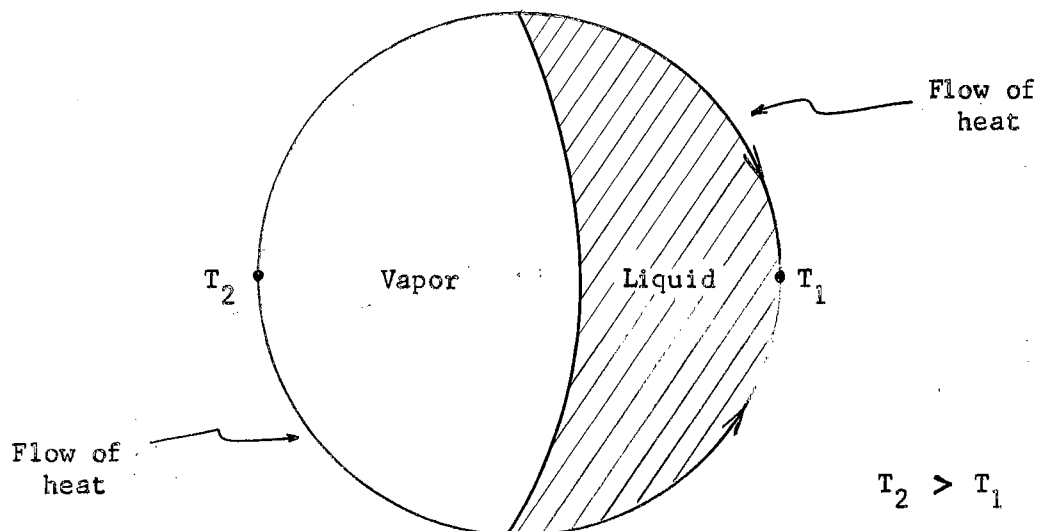


Figure 5. Temperature Difference in a Cross-Section of the Tubing

will be superheated. The difference between T_2 and T_1 might be great when using fixed heat flux heater. It should be mentioned that in such a case heat will flow from the high temperature area of the tubing to the low temperature area as shown in Figure 5. Useful information on this point would be obtained by measuring the temperatures T_1 and T_2 along the coil.

Boiling Heat Flux Determination

The coil can be divided into the following three sections, according to the state of the fluid: preheating section, boiling section and vapor superheating section. By heat balance the heat loads q_{PH} , q_B and q_{SH} can be evaluated. There is no way to calculate the heat transferred by subcooled boiling and it is included in the preheating heat load. The boiling section is taken as the section in which the liquid boils regardless of the specific boiling mechanism which might take place in the various parts of the boiling section. As stated previously, the heat transfer area between the liquid and the wall surface changes continuously as the boiling mixture progresses up the coil. In evaluating the boiling heat flux, the apparent area, i.e. the entire inner surface of the coil in the boiling section will be considered.

The liquid preheating heat transfer area, A_{PH} and the vapor superheating area A_{SH} can be calculated using the respective apparent over-all mean temperature differences between the steam and the liquid or vapor. The coefficients can be calculated using the Sieder-Tate and Dittus-Boelter correlations.

The boiling heat transfer area A_B and thence the boiling heat flux $(q/A)_B$ is then obtained by subtracting A_{PH} and A_{SH} from the total coil

inner surface (see Appendix B).

Experimental Testing of the Theoretical Model

In this work only part of the assumptions outlined in this chapter can be tested. There is no means to check the effect of the radial acceleration on $(q/A)_{mic}$ with the available apparatus. Since this effect is believed to be small compared to the effect of the radial acceleration on $(q/A)_{mac}$, only the over-all change in boiling heat flux will be examined.

It is impossible to differentiate between the mixture velocity and the radial acceleration, because their effects on boiling are superimposed, therefore the boiling heat fluxes will be correlated for a/g and for G separately. The temperature difference between the tube wall on the vapor side, T_2 and that on the liquid side, T_1 (see Figure 5) will give a strong indication of the existence of two separate-phase flow. The existence of two separated phases flowing inside the coil is a key assumption in this model (see Figure 4) since de-entrainment will take place only when two separated phases exist. At high quality the liquid deficiency zone is greater than at low quality, and consequently the de-entrainment effect is expected to be more substantial in the former; therefore measurements of boiling heat fluxes will be conducted in two separate series, i.e. low and high quality. The theoretical model presented in this chapter gives a qualitative model of boiling of a fluid inside a coil. In order to verify this model quantitatively a more sophisticated apparatus than used in this work is required, (see Chapter V and recommendations in Chapter VIII). The experimental procedure and measurements are given in details in Chapter VI.

CHAPTER V

EXPERIMENTAL APPARATUS

The test apparatus was constructed to investigate the behaviour of boiling water and n-hexane in a coil using condensing steam as the heat source.

The apparatus consisted of a boiler shell, a copper coil for the test section, a shell and tube type condenser, liquid surge tank, connecting piping and dry steam supply. A flow diagram is shown in Figure 6.

Boiler shell (see Figure 8 and Figure 9)

material: steel

dimensions: height 3 feet 1-1/16 inches

O. D. 10-3/4 inches.

The shell was supported by a steel frame, see Figure 9.

Copper Coil

tubing: 1/2 inch BWG type K (soft) copper.

total tubing length: 23 feet 10-1/4 inches

coil dimensions: outside diameter 7-1/8 inches

height 2 feet 6 inches

Thermocouple

Twelve copper-constantan thermocouples were placed in pairs, at several points along the tubing (see Figure 7). The thermocouple pairs were 20 inches apart. One of the pair was soldered on the

inside of the coil (called vapor side) and the other on the outside of the coil (called liquid side). Each thermocouple was placed into a small groove made in the tubing wall. The depth of the groove was about one-half of the wall thickness.

The thermocouples were copper-constantan, gauge 20, Servo-Rite No. T24-2-504, Claud S. Gordon Co., insulated with double nylon coating. The thermocouples were connected through two selector multi-switches to a portable Leeds and Northrup potentiometer cat. no. 8686.

Auxiliary Equipment

Pump: A centrifugal pump driven by an 1/8 HP electric motor forced the test fluid through the coil.

Container: A five-gallon container was used to hold the liquid being circulated (see Figure 13).

Condenser: A 1:1 shell and tube exchanger using tap water as the cooling fluid in the tubes, condensed and subcooled the test fluid, (see Figure 13).

Pressure gauge: A bourdon type pressure gauge, 0 psig to 60 psig range, was used to measure the pressure at the boiling liquid inlet, (see Figure 10).

Flow meters: A rotameter was used to measure the test liquid flow rate. An orifice and a U-tube manometer were used to measure cooling water flow rate to the condenser, (see Figure 9).

Thermometers: Eight mercury thermometers with temperature range of 25 degrees F to 240 degrees F were used to record the inlet and outlet temperatures of boiling liquid, steam, condensate and condenser cooling

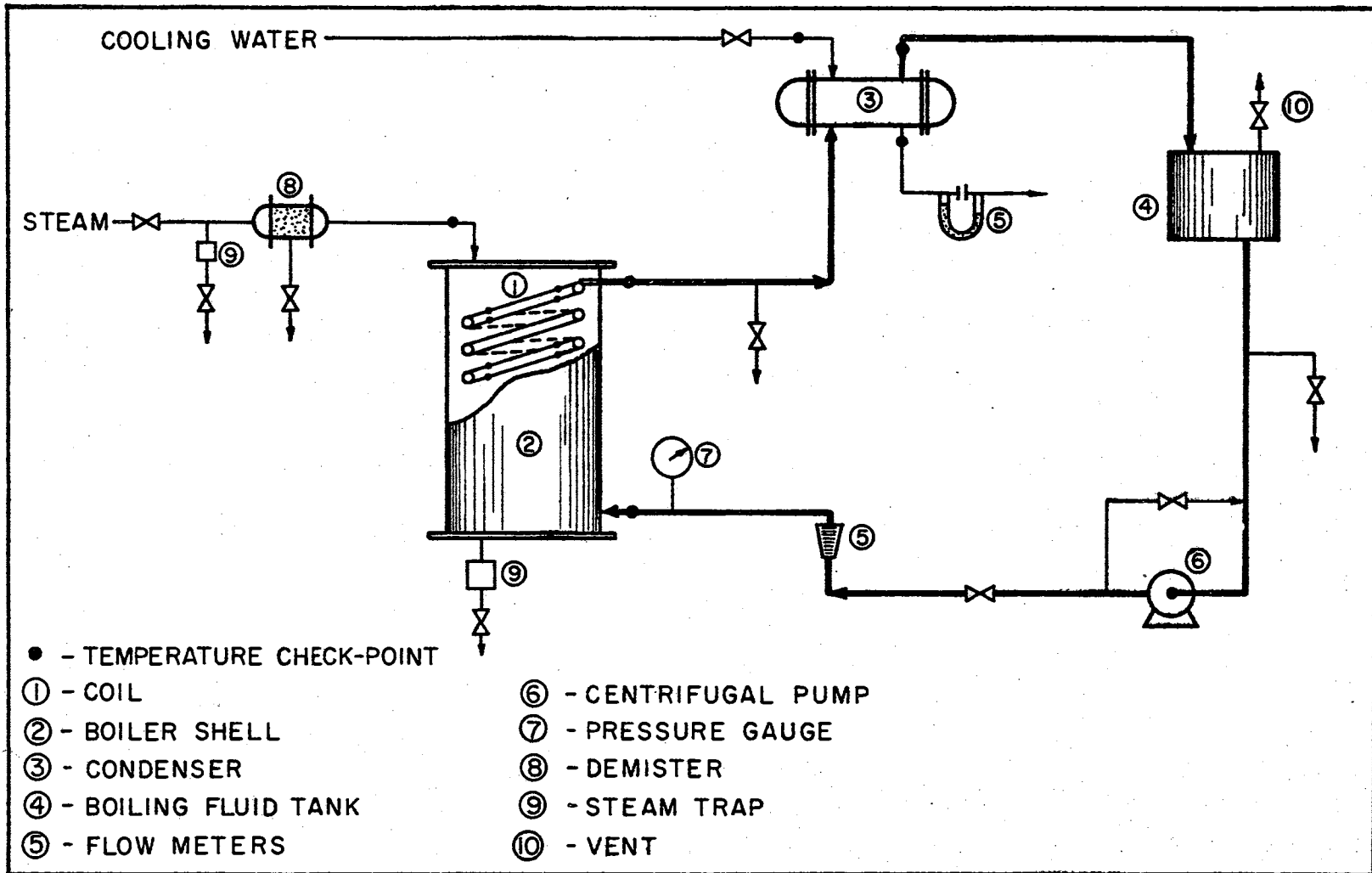


Figure 6. Flow Sheet Diagram.

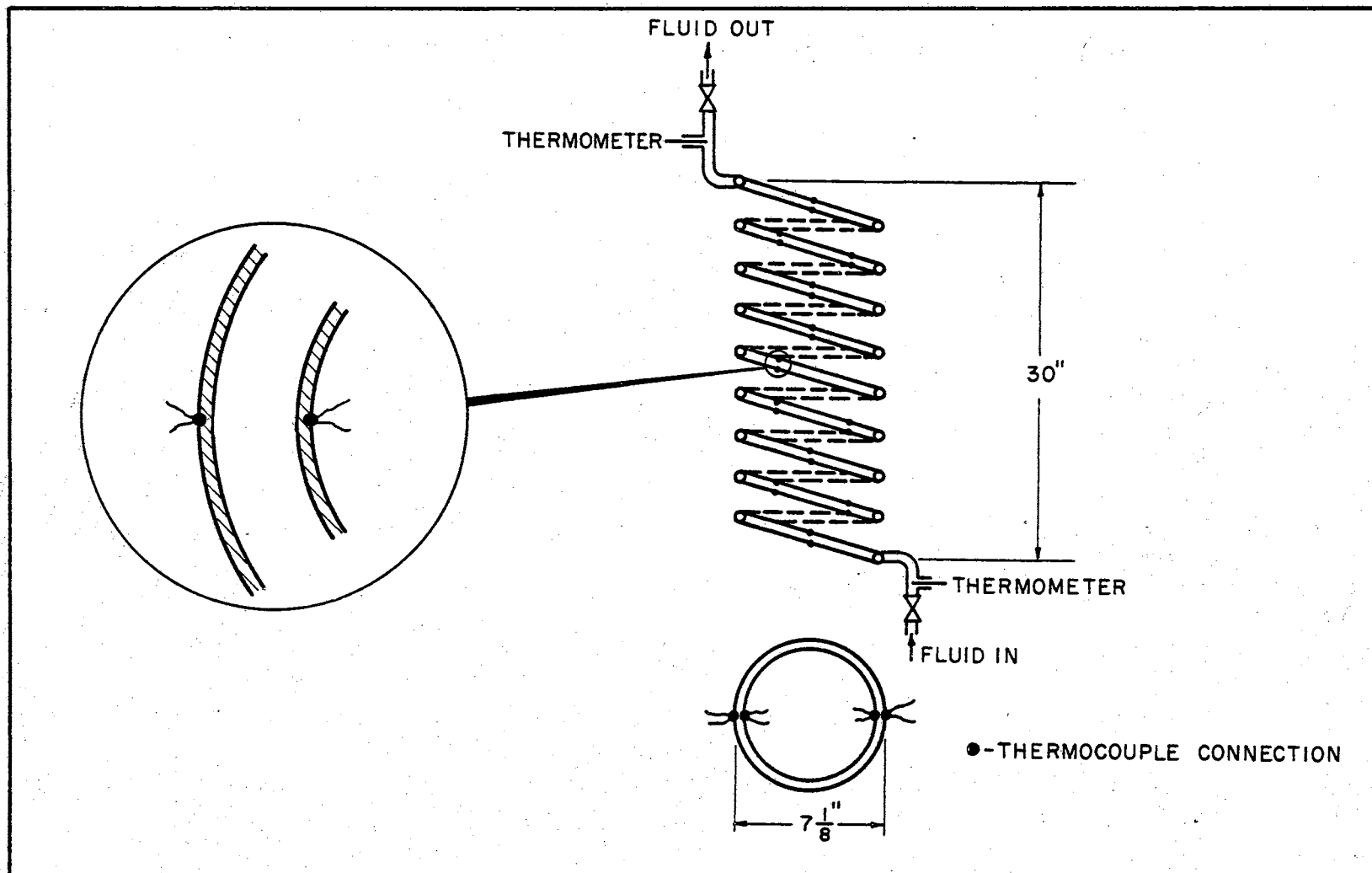


Figure 7. The Coil and the Thermocouple Connections

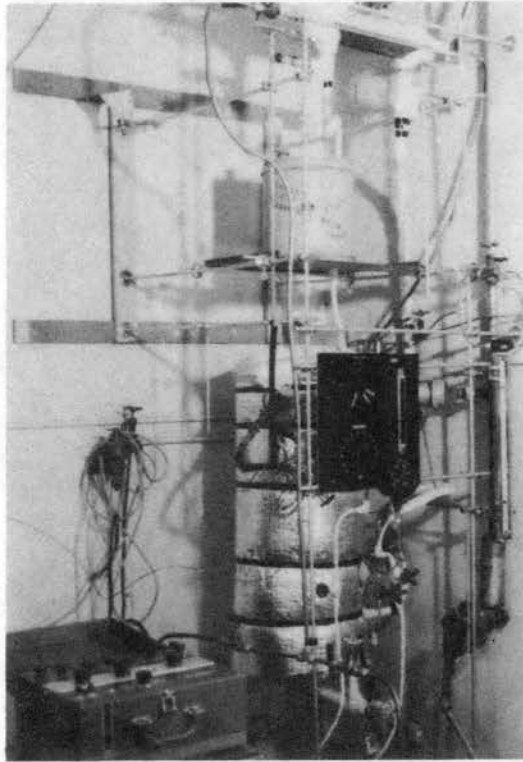


Figure 8. General View of Apparatus
and Auxiliary Equipment.

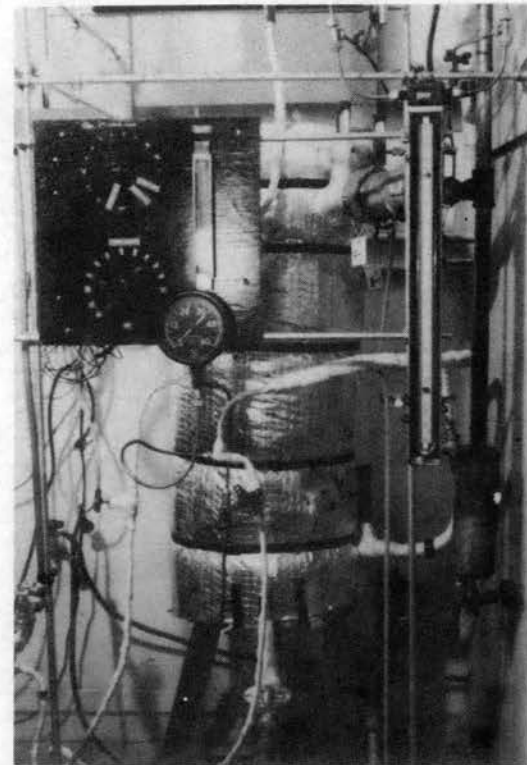


Figure 9. Boiler Shell, Steam Demister
and Flow Meters.

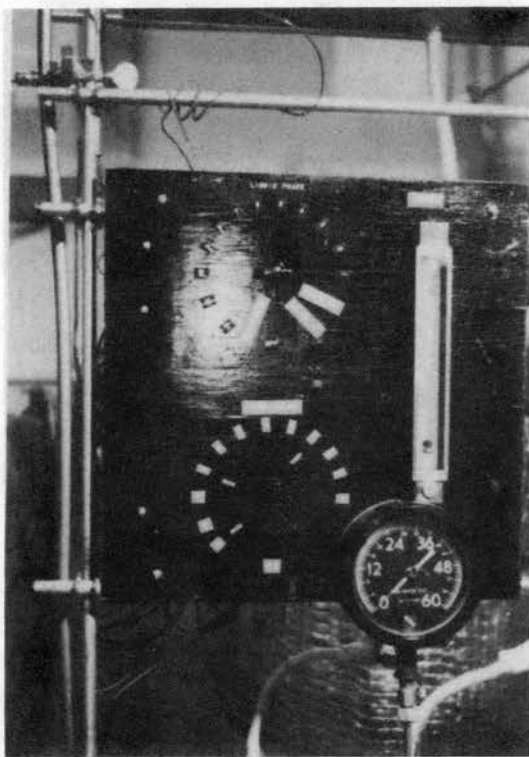


Figure 10. Instrument Panel

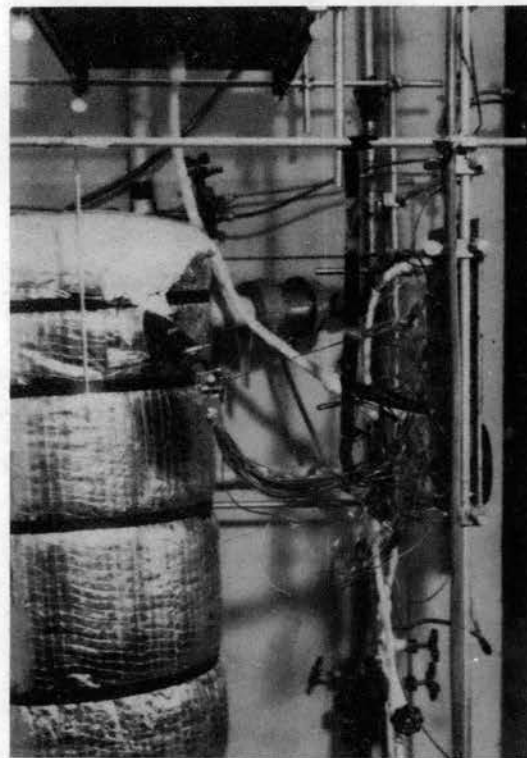


Figure 11. Boiler Shell Insulation
and Thermocouple Wiring.

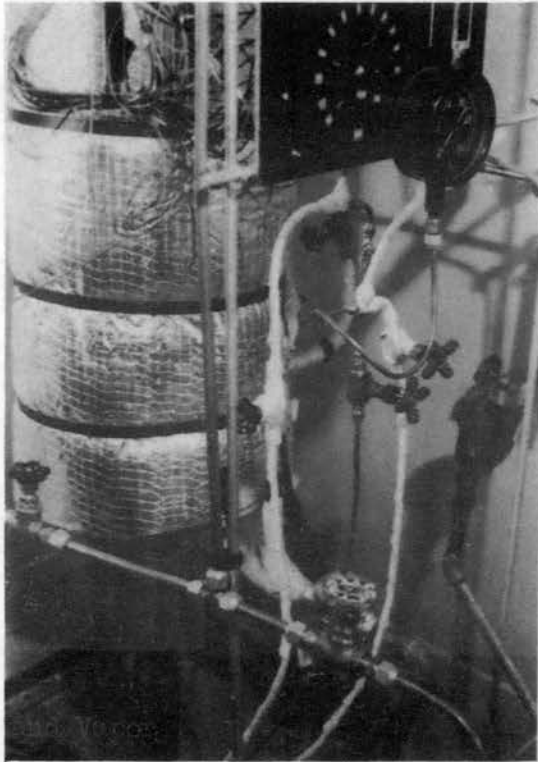


Figure 12. Piping.

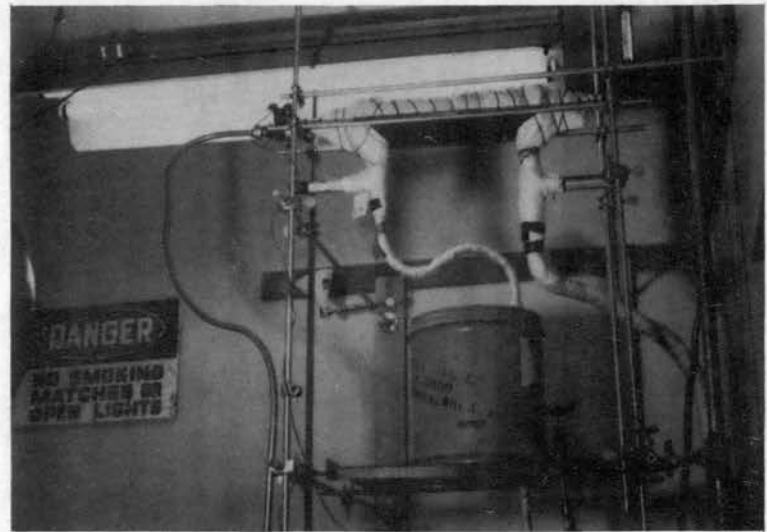


Figure 13. Boiling Fluid Tank and Vapor Condenser.

water.

Insulation: The shell boiler was insulated by two layers of fiber glass mats and insulating cement, (see Figure 11). The condenser and all the pipes were insulated with fiber glass tape, (see Figure 12).

CHAPTER VI

EXPERIMENTAL PROCEDURE

The rotameter, the orifice flow meter and the thermocouples had been previously calibrated (see Appendix D).

Start-Up Procedure

Before beginning the experimental work the system was thoroughly checked for leakage. When the apparatus and all the auxiliary instruments were found to function properly, the system was operated for three successive days in order to age the copper tubing in an attempt to reduce variation in surface texture and scale deposit which might affect the boiling inside the coil and the condensation of steam outside it. The heat losses of the system were estimated by heating up the system to the working temperature in absence of the boiling liquid and measuring the amount of condensate per unit time.

After the steam valve had been opened and the system had been heated for an hour the condenser cooling water valve and the boiling liquid valve were opened. The cooling water flow was adjusted to get at least 10 degrees F subcooled liquid in the case of n-hexane for precaution reasons.

After the boiling liquid had been flowing for half an hour the system was checked for steady-state as following: flows and temperatures were recorded every two to three minutes for the next 30 minutes. The

steady-state criterion was: no variation in at least six successive sets of measurements during a period of at least 15 minutes, (after the system had been running for 45 minutes).

All measurements reported in this thesis were recorded after steady-state conditions had been obtained.

Measurement and Data Recording Procedure

The following measurements were made and recorded

- (a) General measurements:
 - 1. Time
 - 2. Room temperature
- (b) Boiling liquid:
 - 1. Flow rate
 - 2. Temperature at boiler inlet
 - 3. Temperature at boiler outlet
 - 4. Temperature at condenser inlet
 - 5. Temperature at condenser outlet
 - 6. Temperature of liquid in tank
- (c) Cooling water:
 - 1. Flow rate
 - 2. Temperature at condenser inlet
 - 3. Temperature at condenser outlet
- (d) Heating steam:
 - 1. Temperature of steam at evaporator inlet
 - 2. Temperature of condensate at evaporator outlet
 - 3. Weight of condensate per hour
- (e) Pressure:
 - 1. Pressure of the boiling liquid at evaporator inlet
- (f) Wall temperatures of the coil:
 - 1. The wall temperatures along the wall were measured by the thermocouples and

the 24 potentiometer readings were recorded.

CHAPTER VII

EXPERIMENTAL RESULTS AND CORRELATED DATA

The experimental program was devised to investigate the boiling of n-hexane and water in a coil heated by condensing steam outside the coil. A summary and discussion of the results are presented in this chapter.

It was discussed in Chapter IV how the self-induced radial acceleration perpendicular to the hot surface might affect the boiling due to the de-entrainment of the liquid and the change in the boiling characteristics. The results given in the following section will show the dependence of liquid outlet temperatures, wall temperature distribution, and boiling heat fluxes upon the liquid flow rates and the linear velocities. In the section after the following the data will be correlated in the light of the theoretical model outlined in Chapter IV.

Experimental Results

Figure 14 shows the increase of outlet temperatures with the increase of flow rate for n-hexane.

In Figure 15 is shown the increase of outlet temperatures with the increase of water flow rate in the range of 5.1 lbs/hr up to 17.5 lbs/hr and complete vaporization, and for water flow rate in the range of 34.5 lbs/hr up to 113.5 lbs/hr and partial vaporization.

Figure 16 and Figure 17 show the relationship between boiling heat fluxes based upon the outside surface of the boiling section of the coil

and flow rates of n-hexane and water, (see Appendix B for a sample calculation for boiling heat fluxes).

Figure 18 shows a typical temperature profile along the coil wall for run no. 4, (see also Appendix A for tabulation of temperature distribution data). The heat balance on the boiling liquid, heating steam and cooling water are given in Tables III and IV in Appendix A.

The pressure at the boiling liquid inlet increased slightly with flow rate. The maximum pressure recorded was 6.0 psig with n-hexane and water at high flow rates, (up to 113.5 lbs/hr), the outlet pressure was nearly atmospheric. The pressure data are plotted versus flow rates in Figure 22 and Figure 23 and given in Table X in Appendix A.

Correlation of Data

The theoretical model described in Chapter IV was formulated to relate the combined influence of the de-entrainment of the liquid and the change in boiling characteristics to the radial acceleration acting on the boiling liquid.

Figure 19 shows the dimensionless radial acceleration versus quality for n-hexane and water.

In Figure 20 are shown the boiling heat fluxes for n-hexane versus dimensionless acceleration computed assuming 50 per cent quality. Figure 21 shows the same for water (Series D).

Experimental Errors

There are two kinds of error involved, those due to uncertainty in the measurements, and inherent error involved in the particular method of calculation used. The experimental errors in the various measurements

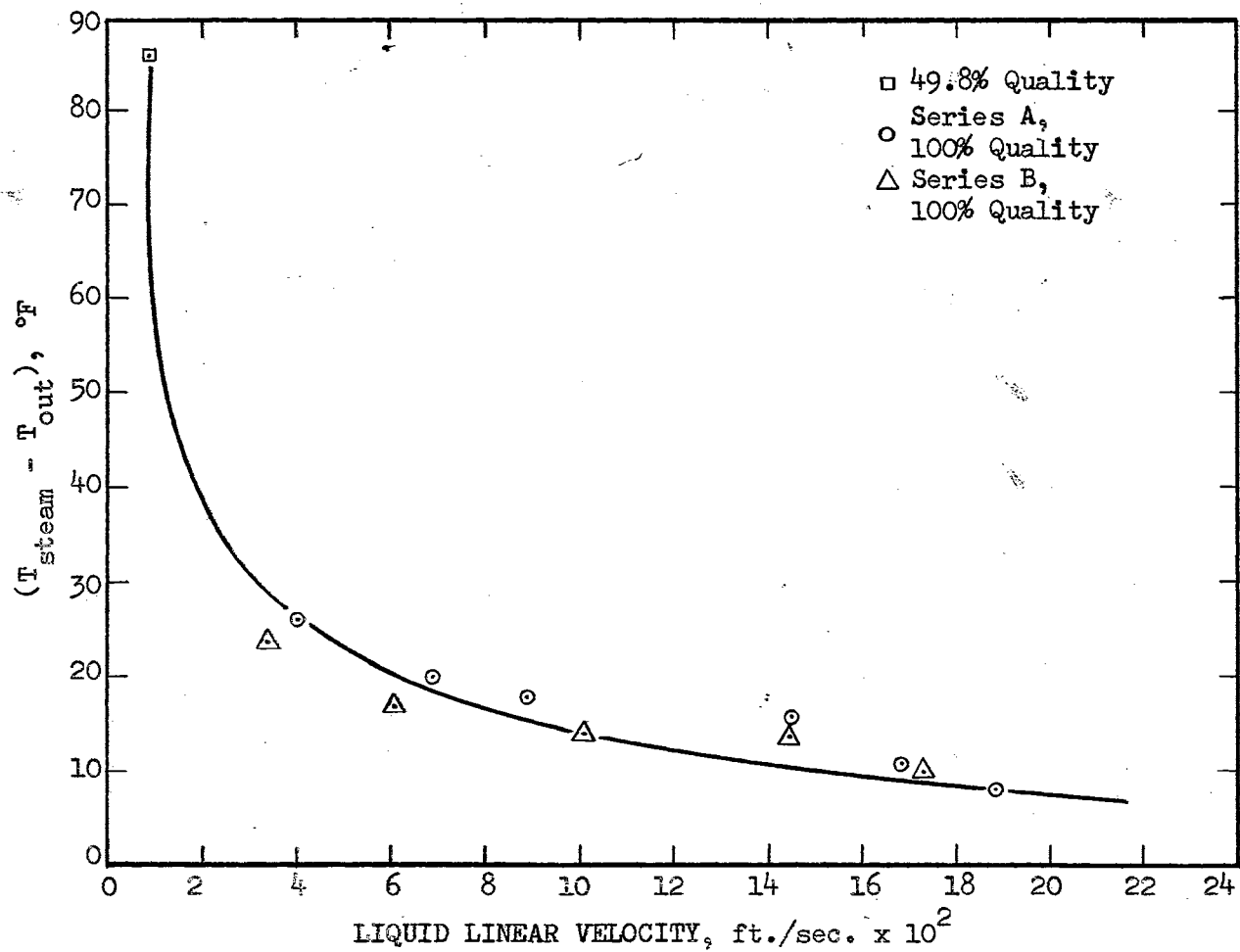


Figure 14. Temperature Difference Between Steam and Outlet Stream for n-Hexane

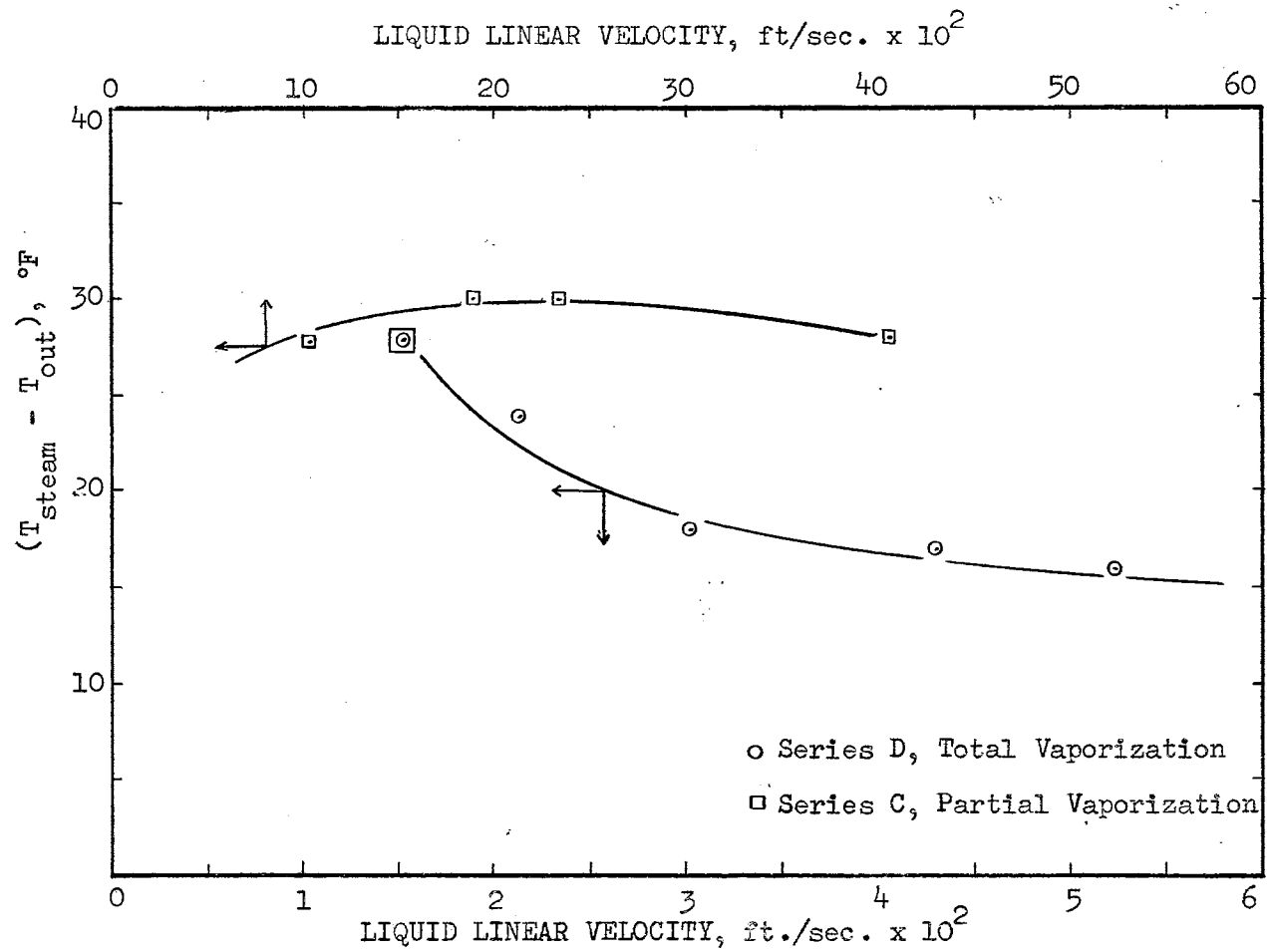


Figure 15. Temperature Difference Between Steam and Outlet Stream for Water

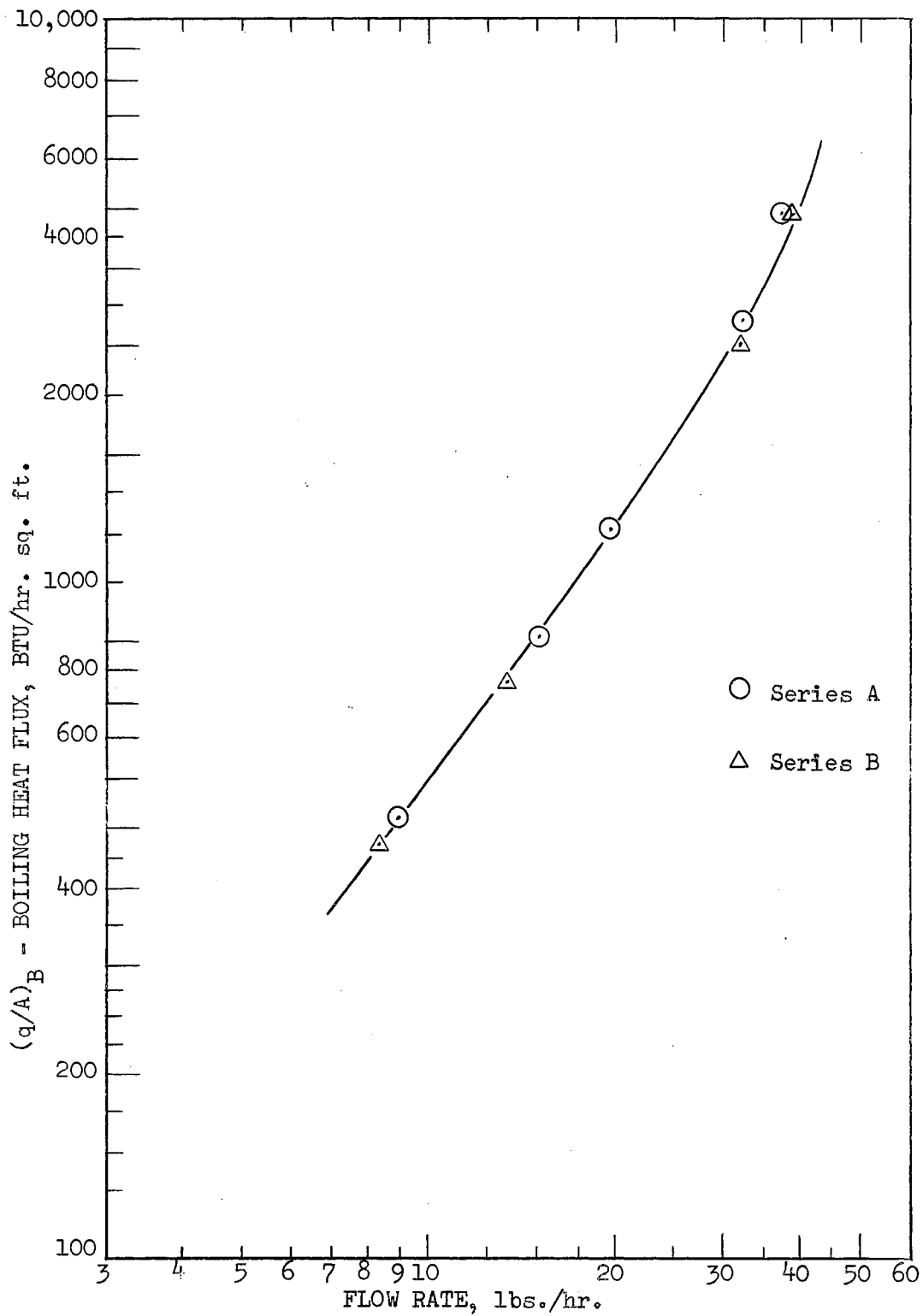


Figure 16. Boiling Heat Flux of n-Hexane Versus Flow Rate

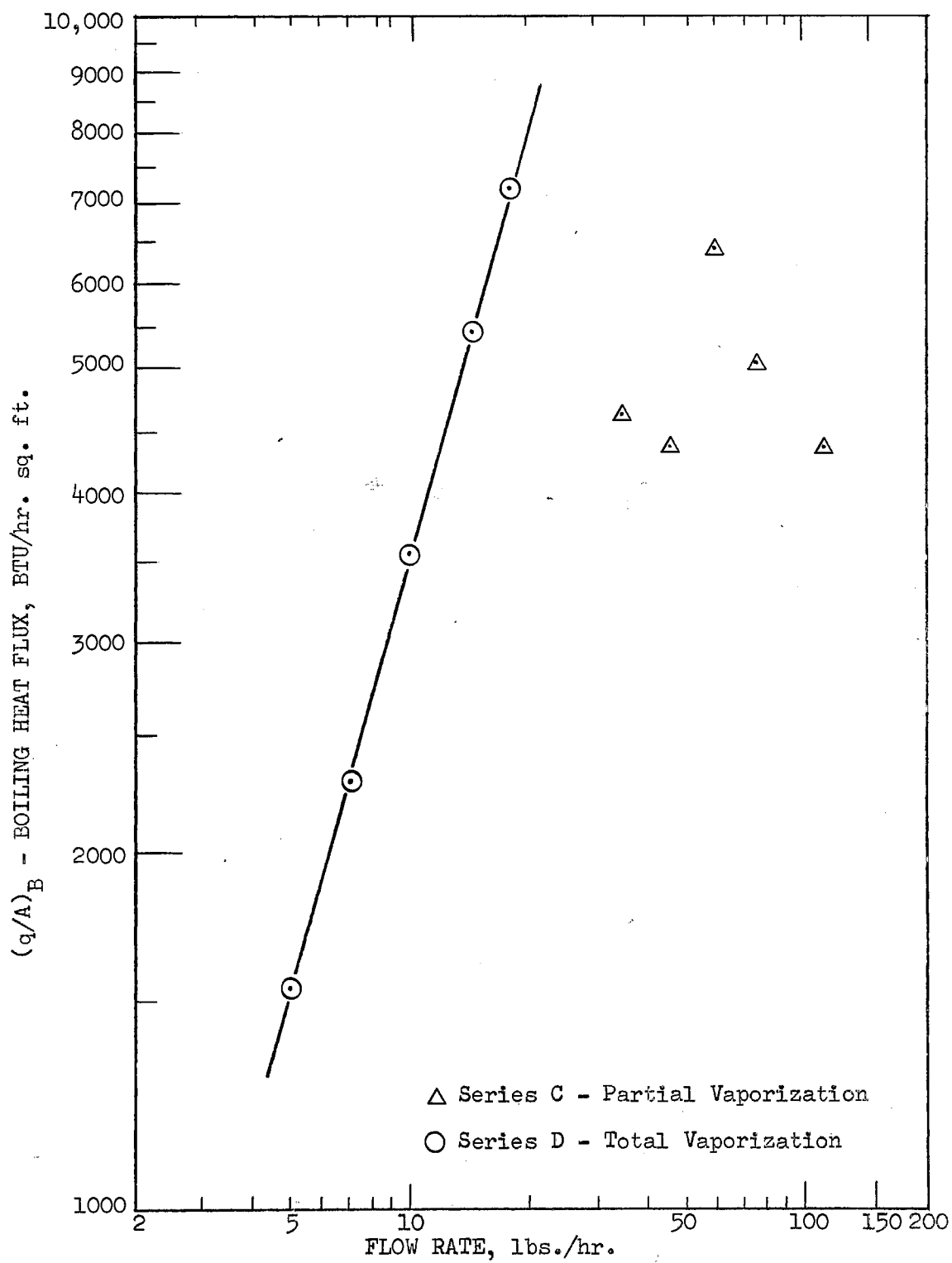


Figure 17. Boiling Heat Flux of Water Versus Flow Rate

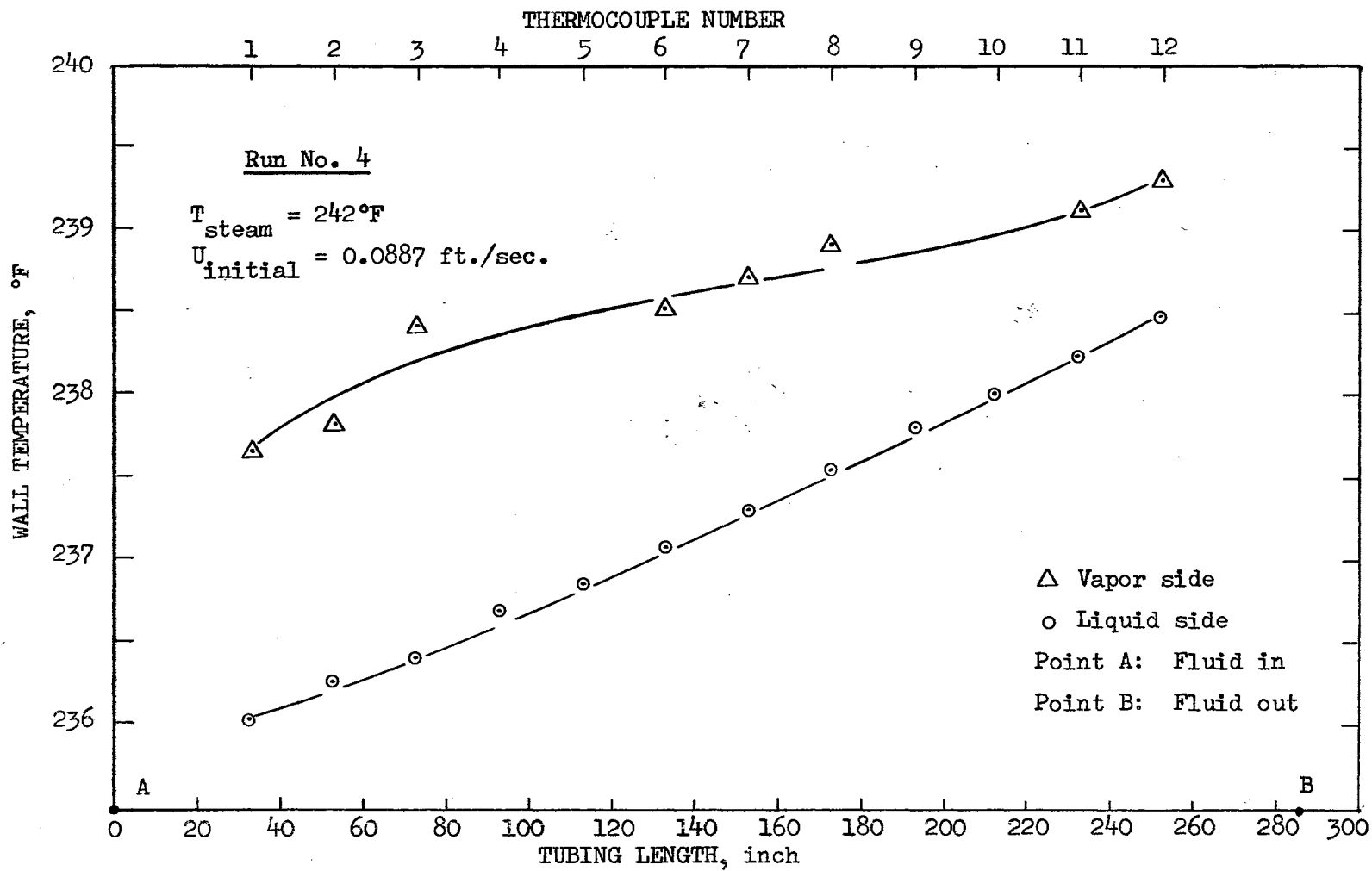


Figure 18. Temperature Profile Along the Coil

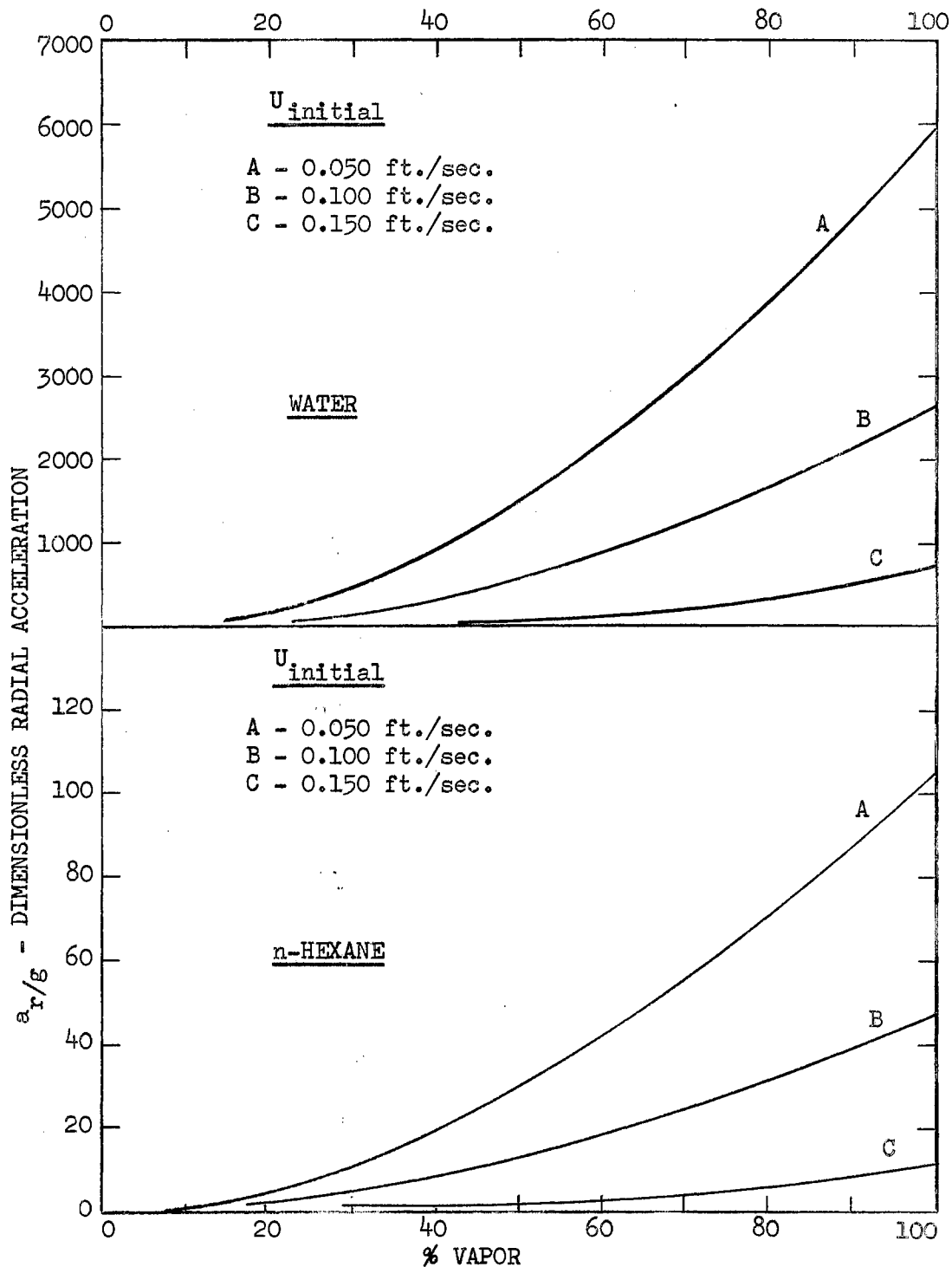


Figure 19. Dimensionless Radial Acceleration Versus Per Cent of Vapor for n-Hexane and Water

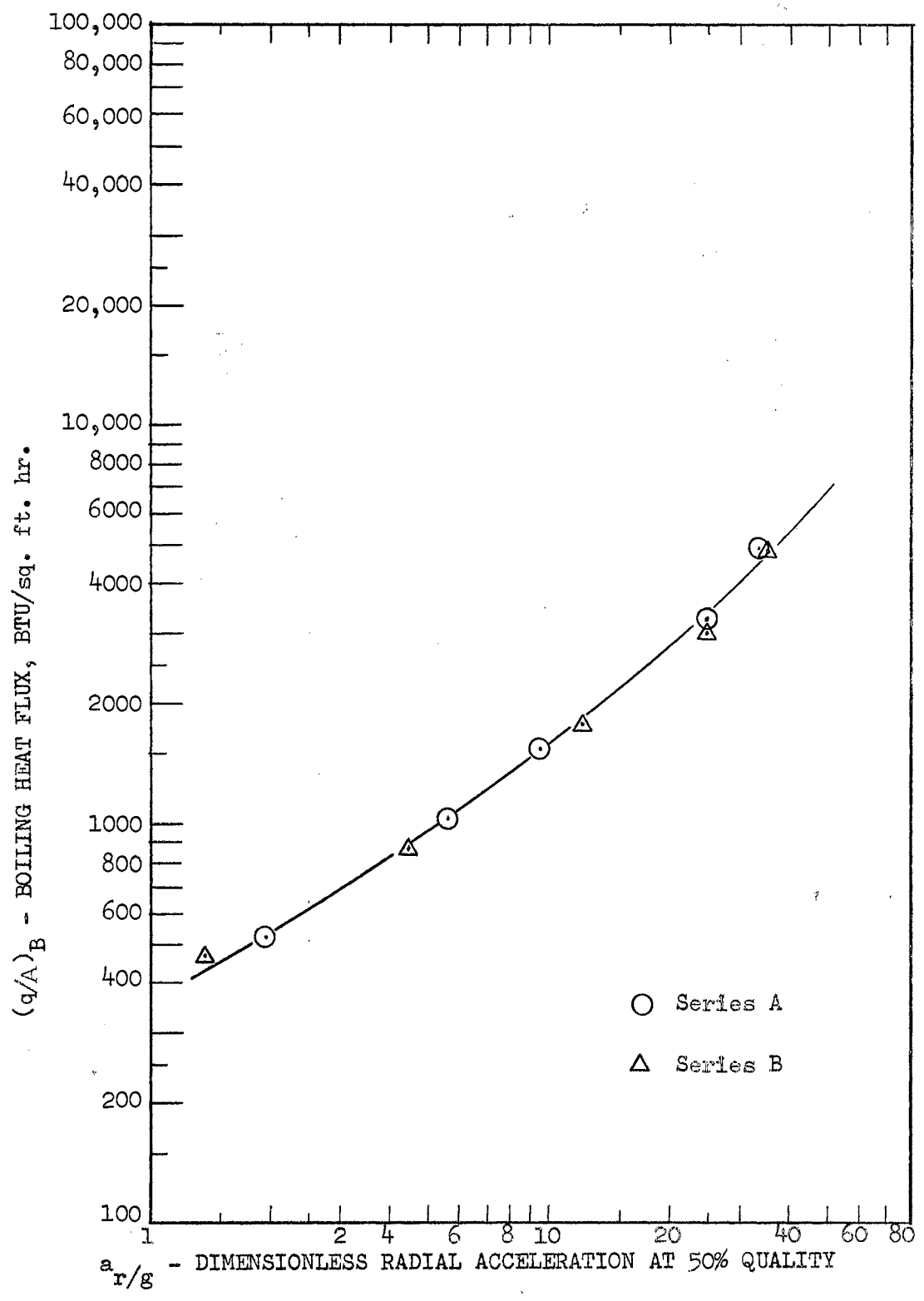


Figure 20. Boiling Heat Flux of n-Hexane Versus Dimensionless Radial Acceleration

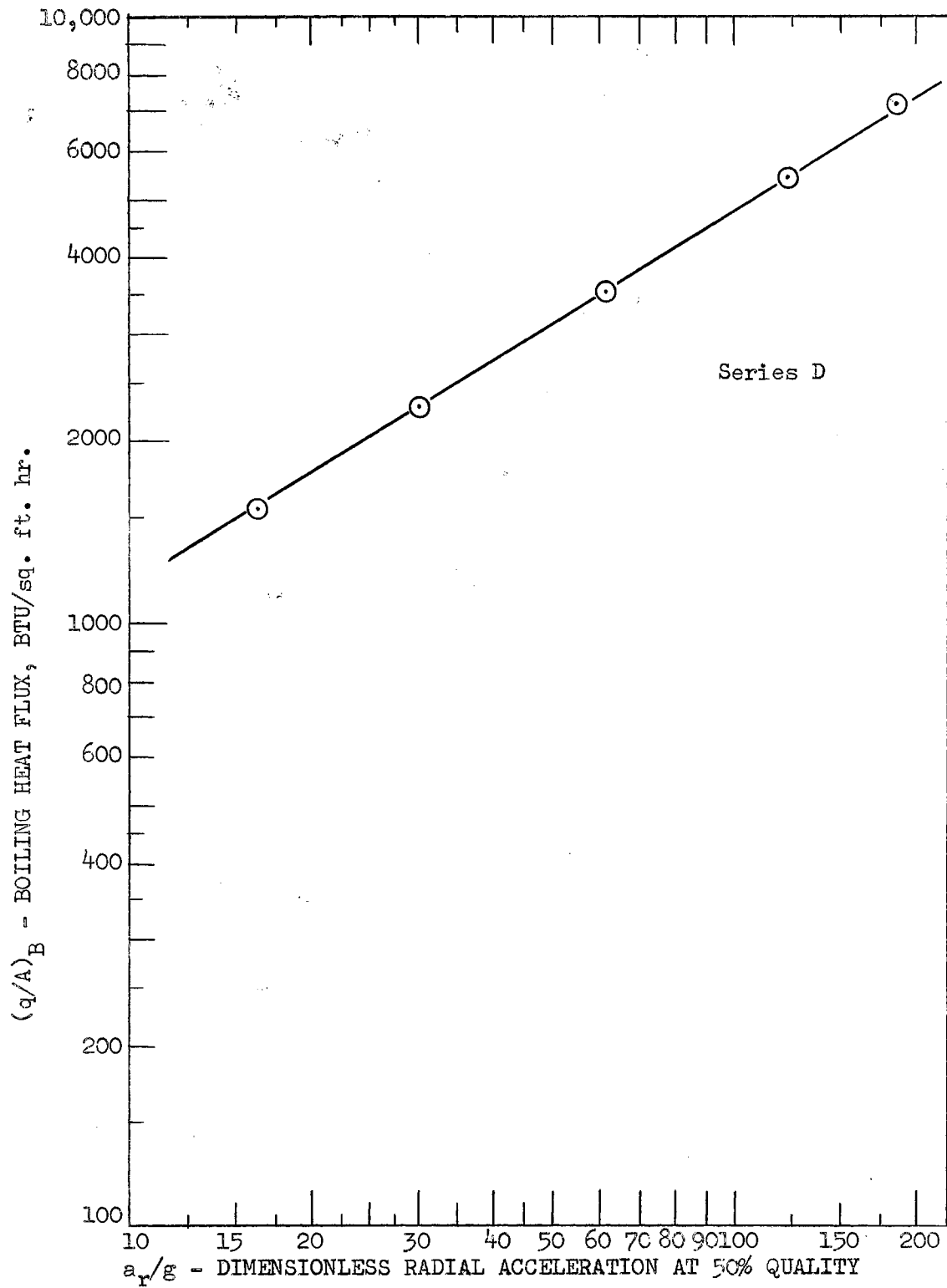


Figure 21. Boiling Heat Flux of Water Versus Dimensionless Radial Acceleration

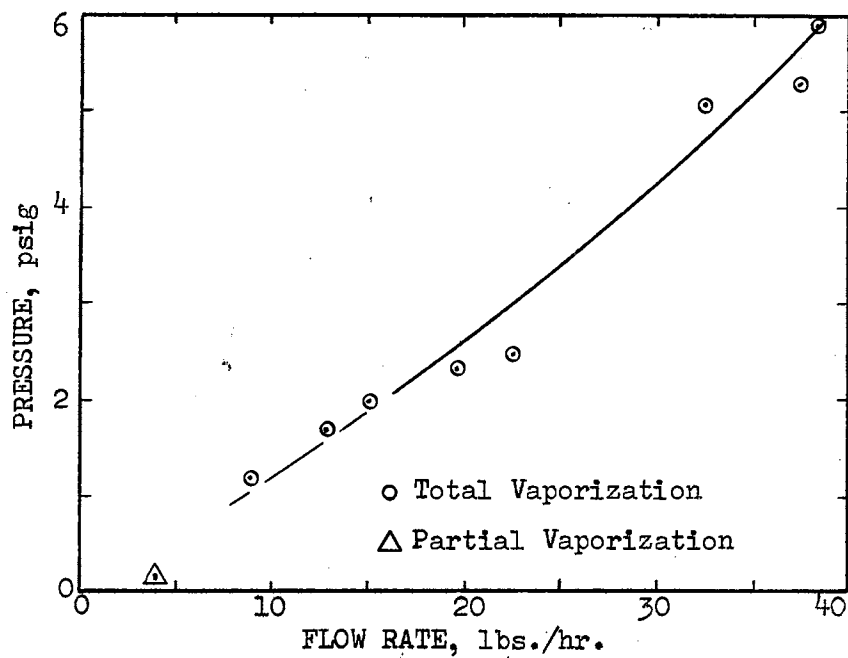


Figure 22. Boiler Inlet Pressure Versus Flow Rate of n-Hexane

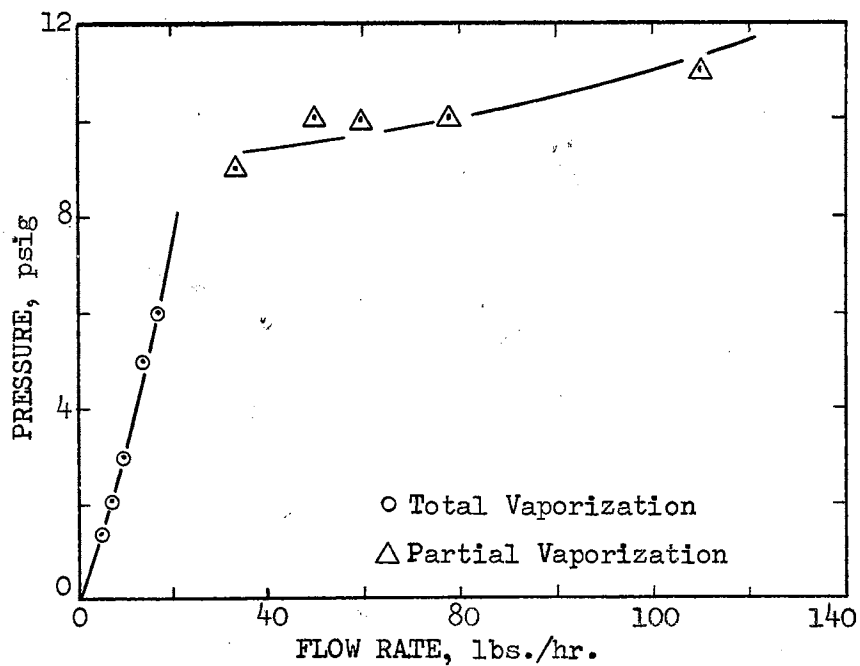


Figure 23. Boiling Inlet Pressure Versus Flow Rate of Water

are the following:

Cooling water: ± 30 lbs/hr

N-hexane flow rate: ± 0.3 lb/hr

Water flow rate: ± 0.3 lb/hr

Mercury thermometer: ± 0.5 degree F

Thermocouple: ± 0.05 degree F

Inlet pressure: ± 0.25 psi

Condensate: 0.110 lb/hr

The absolute maximum error interval as a result of the above experimental error are:

Steam enthalpy: ± 105 BTU/hr

q_B for n-hexane: ± 42.5 BTU/hr

q_B for water: ± 291 BTU/hr

Inherent error. The heat transfer areas for preheating and superheating were calculated via the Sieder-Tate correlation (for laminar flow $Re < 2100$) and Dittus-Boelter correlation for turbulent flow. The accuracy of those correlations are ± 25 per cent. This introduces an uncertainty in all the boiling heat transfer areas A_B and consequently in the boiling heat flux, $(q/A)_B$.

CHAPTER VIII

DISCUSSION OF RESULTS, CONCLUSIONS AND RECOMMENDATIONS

It has been determined experimentally that when liquid n-hexane and water flow under boiling conditions through a coiled copper tubing heated by steam the boiling heat flux increased with flow rate for n-hexane in the range of 4.2 lbs/hr to 37.5 lbs/hr and for water in the range of 5.1 lbs/hr to 17.5 lbs/hr. For water at flow rates range of 34.5 lbs/hr to 113.5 lbs/hr the change of boiling heat flux did not follow the same pattern.

It was also shown that for the n-hexane runs and for water runs in the range of 5.1 lbs/hr to 17.5 lbs/hr at 100 per cent quality the temperature of the superheated vapor leaving the coil increased with increase of flow rate. Temperature differences between the vapor side and liquid side, though small were recorded for all the runs, (see Appendix A). The above might indicate strongly that two separate phase flow does exist in boiling in a coil.

Sufficient data are not available from the present work to make generalized conclusions as to the role of the radial acceleration on boiling at low quality, nor to obtain a quantitative picture for high quality. However the substantial increase of boiling heat fluxes at 100 per cent vapor, and the increase of superheating temperatures with increase of flow rate for n-hexane and water runs strengthen the assumption that de-entrainment of the dispersed liquid in the liquid deficient zone

is of prime importance especially at high quality.

The relatively small boiling heat fluxes in water runs of series "C," might be explained by the pressure drops (9.0 psig to 11.0 psig) in these runs, (see Table X). The higher pressure tends to increase the saturation temperature and thus suppresses the boiling.

It is the feeling of the experimenter that at very high radial acceleration and moderate vapor quality, the influence of the acceleration on the boiling characteristics (such as vapor bubble diameter and velocity at its departure from the wall) predominates, and that the boiling heat transfer in this case is adversely affected by the acceleration.

In nucleate boiling the increased buoyancy force will increase the initial velocity of the bubble but will decrease its size at the departure from the hot surface. Thus there should be some optimum acceleration from the standpoint of heat transfer behavior at which the net improvement of boiling heat transfer is maximized.

It can be concluded that the main advantage of radial acceleration in boiling inside a coil is through changing the flow characteristics rather than the boiling characteristics.

If the increase in boiling heat flux at 100 per cent vapor quality is attributed solely to the increase in radial acceleration, then the data obtained indicate the following:

For n-hexane:

$$(q/A)_B \propto (a/g)^{0.770 - 0.835}$$

For water:

$$(q/A)_B \propto (a/g)^{0.620}$$

In terms of flow rates the data indicate:

For n-hexane:

$$(q/A)_B \propto (G)^{1.545 - 1.580}$$

For water in flow rate range of 5.1 lbs/hr to 17.5 lbs/hr:

$$(q/A)_B \propto (G)^{1.265}$$

Recommendations

It is recommended that the following studies will be carried out in the future:

- (1) Photographic and visual study of boiling in a coil using an electrically-heated coil made out of electrical-conductive glass (manufactured by Corning Glass Works, Corning, N. Y.) as heat source, and a dyed liquid as the test fluid. In this study the various flow regimes and the two-separate phase flow could be observed and photographed.
- (2) An experiment using an electrically-heated coil as heat source. In this kind of experiment the local heat fluxes can be measured accurately.

Industrial applications of an apparatus of this kind or similar might be considered after the technical and economic aspects have been studied thoroughly.

BIBLIOGRAPHY

1. Bonilla, C. F., and C. H. Perry. Trans. Am. Inst. Chem. Engr., 37 (1941), 685.
2. Bromley, L. A. Chem. Engr. Progr., 46 (1950), 221.
3. Bromley, L. A., N. R. LeRoy, and J. A. Robbers. Indust. Engr. Chem., 45 (1953), 2639.
4. Cichelli, M. T., and C. F. Bonilla. Trans. Am. Inst. Chem. Engr., 41 (1945), 755.
5. Cole, R. Am. Inst. Chem. Engr., 6 (1956), 533.
6. Costello, C. P., and J. M. Adams. Intern. Development in Heat Transfer, 2 (1961), 255.
7. Costello, C. P., and W. E. Thuthill. Chem. Engr. Progr. Symp. Series No. 32, 57 (1961), 189.
8. Costello, C. P., and J. M. Adams. Am. Inst. Chem. Engr., 5 (1963), 663.
9. Cryder, D. S., and A. C. Finalborgo. Trans. Am. Inst. Chem. Engr., 33 (1937), 346.
10. Drew, T. B., and A. C. Mueller. Trans. Am. Inst. Chem. Engr., 33 (1937), 449.
11. Forster, H. K., and N. J. Zuber. Jour. Appl. Phys., 25 (1954), 474.
12. Forster, H. K. Jour. Appl. Phys., 25 (1954), 1067.
13. Forster, H. K., and N. J. Zuber. Am. Inst. Chem. Engr., 1 (1955), 531.
14. Forster, H. K., and R. Greif. Jour. Heat Trans., 81 (1959), 43.
15. Gambill, W. R., and N. D. Greene. Chem. Engr. Progr., 10 (1958), 69.
16. Gambill, W. R. British Chem. Engr., 8 (1963), 93.
17. Gambill, W. R. Chem. Engr. Progr. Symp. Series No. 41, 59 (1963), 71.
18. Insinger, T. H., and H. Bliss. Trans. Am. Inst. Chem. Engr., 36

(1940), 491.

19. Ivey, H. J. Paper submitted to the Inst. Mech. Engr., London, England (April 1961).
20. Jakob, M. Mech. Engr., 58 (1936), 643.
21. Jakob, M. "Heat Transfer," Vol. 1. New York: Wiley, 1949, Chapter 29.
22. Lang, C. Trans. Inst. Engr. Shipbuilders, Scotland, 32 (1888), 279.
23. Leidenfrost, J. G. "De Aqae Communis Nonnullis Qualitatibus Tractatus." In translation, "A Tract About Some Qualities of Common Water." Sections 15 to 35 translated by C. Wares, University of Oklahoma, Norman, Oklahoma. See also (10) for discussion on this publication.
24. Lowery, W. J., and J. W. Westwater. Indust. Engr. Chem., 49 (1957), 1445.
25. McFadden, P. W., and P. Grassman. Intern. Jour. Heat and Mass Trans., 5 (1962), 169.
26. McNelly, M. J. Imperial College Chem. Engr. Soc., 7 (1953), 18.
27. Mead, B. R., F. E. Romie, and A. G. Guibert. "Heat Transfer and Fluid Mechanics." Stanford: Stanford U. P., 1951, p. 209.
28. Merte, H., Jr., and J. A. Clark. Jour. Heat Trans. (1961), 233.
29. Nukiyama, S. Soc. Mech. Engr., Japan, No. 206, 37 (1934), 267.
30. Rohsenow, W. M., and J. A. Clark. Trans. Am. Soc. Mech. Engr., 73 (1951), 609.
31. Rohsenow, W. M. Trans. Am. Soc. Mech. Engr. 74 (1952), 969.
32. Rohsenow, W. M., and H. Y. Choi. "Heat Mass and Momentum Transfer." Englewood, New Jersey: Prentice-Hall Inc., 1961.
33. Siegel, R., and C. M. Usiskin. Am. Soc. Mech. Engr. Jour. Heat Trans. (1959), 230.
34. Siegel, R., and E. G. Keshock. Am. Inst. Chem. Engr., 4 (1964), 509.
35. Usiskin, C. M., and R. Siegel. Jour. Heat Trans. (1961), 243.
36. Westwater, J. W., and J. G. Santangelo. Indust. Engr. Chem., 47 (1955), 1605.
37. Zuber, N. J. Trans. Am. Soc. Mech. Engr. 80 (1958), 711.

APPENDIX A

EXPERIMENTAL AND CALCULATED DATA

TABLE I
FLOW RATES AND TEMPERATURES DATA FOR N-HEXANE

Run No.	Flow Rate lbs/hr	Liquid Inlet Velocity-ft/sec	T _{in} °F	T _{out} °F	T _{steam} °F	T _{steam} -T _{out} °F
<u>Series A:</u>						
1	4.2	0.0188	83	156	242	86
2	9.0	0.0403	88	216	242	26
3	15.3	0.0685	98	224	244	20
4	19.8	0.0887	94	224	242	18
5	32.4	0.1450	99	226	242	16
6	37.5	0.1680	105	229	240	11
7	42 *	0.1885 *	99	234	242	8
<u>Series B:</u>						
8	8.4	0.0339	108	218	242	24
9	13.6	0.0609	111	225	242	17
10	22.5	0.1010	109	226	240	14
11	32.4	0.1450	116	228	242	14
12	38.7	0.1730	114	230	240	10

*Approximately

TABLE II

FLOW RATES AND TEMPERATURES DATA FOR WATER

Run No.	Flow Rate lbs/hr	Liquid Inlet Velocity-ft/sec	T _{in} °F	T _{out} °F	T _{steam} °F	T _{steam} -T _{out} °F
<u>Series C:</u>						
13	34.5	0.1030	172	212	240	28
14	50.5	0.1514	185	212	240	28
15	63.0	0.1890	164	212	242	30
16	78.0	0.2340	166	212	242	30
17	113.5	0.4040	168	212	240	28
<u>Series D:</u>						
18	5.1	0.0153	180	216	244	28
19	7.2	0.0216	154	218	242	24
20	10.2	0.0303	154	222	240	18
21	14.4	0.0431	168	223	240	17
22	17.5	0.0525	165	224	240	16

TABLE III
HEAT BALANCE DATA FOR N-HEXANE

Run No.	Flow Rate lbs/hr	Enthalpy - Hexane	Enthalpy - Steam	BTU/hr Cooling Water	% Vapor in Outlet
<u>Series A:</u>					
1	4.2	-	510		49.8
2	9.0	1970	2190		100
3	15.3	3310	2975		100
4	19.8	4531	4200		100
5	32.4	7010	6545		100
6	37.5	8025	7835		100
7	42 *	-	-		100
<u>Series B:</u>					
8	8.4	1724	2260	2170	100
9	13.6	2380	3030	2960	100
10	22.5	4720	4940	4760	100
11	32.4	6675	6300	6340	100
12	38.7	8070	7920	7720	100

*Approximately

TABLE IV
HEAT BALANCE DATA FOR WATER

Run No.	Flow Rate lbs/hr	Water	Enthalpy - Steam	BTU/hr Cooling Water	% Vapor in Outlet
<u>Series C:</u>					
13	34.5		16,000	15,300	44.0
14	50.5		14,500	14,370	27.0
15	63.0		16,600	16,150	22.2
16	78.0		16,200	15,850	16.6
17	113.5		16,700	17,020	10.5
<u>Series D:</u>					
18	5.1	5,130	5,250	5,200	100
19	7.2	7,440	7,600	7,100	100
20	10.2	10,572	10,700	10,800	100
21	14.4	14,730	14,900	14,500	100
22	17.5	17,976	18,100	18,100	100

TABLE V
HEAT TRANSFER DATA--N-HEXANE

Run No.	Flow Rate lbs/hr	Liquid Re	Pr	q_{PH} BTU/hr	q_{SH} BTU/hr	q_B BTU/hr	A_B sq ft	$(q/A)_B$ BTU/sq ft hr
<u>Series A:</u>								
1	4.2	198	4.25	207	-	303	3.126	97.2
2	9.0	426	4.24	415	250	1,305	2.490	525
3	15.3	725	4.20	605	485	2,220	2.170	1,022
4	19.8	936	4.21	837	624	2,870	1.878	1,520
5	32.4	1,530	4.20	1,260	1,050	4,700	1.420	3,310
6	37.5	1,780	4.10	1,310	1,275	5,440	1.110	4,900
<u>Series B:</u>								
8	8.4	397	4.10	266	240	1,218	2.571	473
9	13.6	645	4.09	420	435	1,975	2.287	865
10	22.5	1,072	4.10	728	722	3,270	1.898	1,730
11	32.4	1,530	4.00	890	1,085	4,700	1.545	3,040
12	38.7	1,830	4.00	1,115	1,335	5,620	1.130	4,980

TABLE VI
HEAT TRANSFER DATA--WATER

Run No.	Flow Rate lbs/hr	Liquid		q_{PH} BTU/hr	q_{SH} BTU/hr	q_B BTU/hr	A_B sq ft	$(q/A)_B$ BTU/sq ft hr
		Re	Pr					
<u>Series C:</u>								
13	34.5	1,370	1.75		-	14,540	3.120	4,660
14	50.5	2,070	1.70		-	13,020	2.990	4,360
15	63.0	2,300	1.85		-	13,430	2.100	6,400
16	78.0	2,380	1.85		-	12,430	2.435	5,120
17	113.5	4,120	1.85		-	11,450	2.630	4,360
<u>Series D:</u>								
18	5.1	191	1.88	175	5	4,950	3.200	1,545
19	7.2	256	2.00	440	20	6,980	3.050	2,280
20	10.2	364	2.00	626	46	9,900	2.740	3,510
21	14.4	522	1.85	678	72	13,980	2.580	5,430
22	17.5	635	1.84	880	96	17,000	2.370	7,180

TABLE VII
 RADIAL ACCELERATION AND BOILING HEAT FLUXES FOR N-HEXANE

Run No.	Flow Rate lbs/hr	a_r/g @ 50% Vapors	$(q/A)_B$ BTU/sq ft hr
<u>Series A:</u>			
1	4.2		97.2
2	9.0	1.95	525
3	15.3	5.60	1,022
4	19.8	9.46	1,520
5	32.4	25.20	3,310
6	37.5	33.90	4,900
<u>Series B:</u>			
8	8.4	1.38	473
9	13.6	4.44	865
10	22.5	12.20	1,730
11	32.4	25.20	3,040
12	38.7	35.85	4,980

TABLE VIII
 RADIAL ACCELERATION AND BOILING HEAT FLUXES
 FOR WATER AT PARTIAL EVAPORATION

Run No.	Flow Rate lbs/hr	Average % Vapors	a_r/g @ Ave. Vapors	$(q/A)_B$ BTU/sq ft hr
<u>Series C:</u>				
13	34.5	22.0	138	4,660
14	50.5	13.50	112.8	4,360
15	63.0	11.10	118	6,400
16	78.0	8.30	101.2	5,120
17	113.5	5.25	120.5	4,360

TABLE IX
 RADIAL ACCELERATION AND BOILING HEAT FLUXES
 FOR WATER AT TOTAL EVAPORATION

Run No.	Flow Rate lbs/hr	a_r/g @ 50% Vapors	$(q/A)_B$ BTU/sq ft hr
<u>Series D:</u>			
18	5.1	16.2	1,545
19	7.2	30.1	2,280
20	10.2	61.5	3,510
21	14.4	124.5	5,430
22	17.5	185.5	7,180

TABLE X
PRESSURES AT BOILER INLET

<u>Run No.</u>	<u>N-Hexane Pressure psig</u>	<u>Run No.</u>	<u>Water Pressure psig</u>
1	0.20	13	9.0
2	1.20	14	10.0
3	2.00	15	10.0
4	2.30	16	10.0
5	5.10	17	11.0
6	5.30	18	1.5
7	-	19	2.0
8	1.0	20	3.0
9	1.75	21	5.0
10	2.50	22	6.0
11	5.00		
12	6.00		

TABLE XI
THERMOCOUPLE READING ALONG THE COIL

n-Hexane

Series A

Thermocouple Reading - mv

Thermocouple No.	Run No. 1		Run No. 2		Run No. 3	
	Liquid Side	Vapor Side	Liquid Side	Vapor Side	Liquid Side	Vapor Side
1	5.048	5.048	4.956	4.968	4.980	4.980
2	5.048	5.048	4.960	4.973	4.986	4.986
3	5.040	5.040	4.965	4.990	4.990	4.995
4	5.038	-	4.976	-	4.994	-
5	5.053	5.030	4.979	4.996	5.000	5.002
6	5.030	5.030	4.984	5.000	5.002	5.004
7	5.028	5.028	4.990	5.010	5.004	5.006
8	5.023	-	4.995	-	5.014	-
9	5.019	-	5.000	-	5.019	-
10	5.015	5.015	5.002	5.034	5.024	5.025
11	5.014	5.014	5.009	5.036	5.030	5.030
12	5.009	-	5.015	-	5.035	-

Thermocouple No.	Run No. 4		Run No. 5		Run No. 6	
	Liquid Side	Vapor Side	Liquid Side	Vapor Side	Liquid Side	Vapor Side
1	4.908	4.950	4.925	4.936	4.954	4.958
2	4.914	4.955	4.930	4.994	4.960	4.962
3	4.918	4.970	4.942	4.960	4.965	4.970
4	4.926	-	4.950	-	4.968	-
5	4.930	4.975	4.960	4.964	4.973	4.974
6	4.935	4.979	4.968	4.970	4.975	4.975
7	4.942	4.984	4.973	4.980	4.981	4.985
8	4.948	-	4.985	-	4.985	-
9	4.955	-	4.980	-	4.992	-
10	4.960	4.990	4.984	4.990	4.996	4.998
11	4.966	4.995	4.988	4.995	5.000	5.000
12	4.972	-	5.000	-	4.004	-

TABLE XI (continued)

Thermocouple No.	<u>Series A</u>		<u>Series B</u>			
	Run No. 7		Run No. 8		Run No. 9	
	Liquid Side	Vapor Side	Liquid Side	Vapor Side	Liquid Side	Vapor Side
1	4.972	4.974	4.984	4.997	4.986	4.990
2	4.975	4.977	4.992	5.010	4.994	5.000
3	4.980	4.985	4.997	5.030	5.010	5.015
4	4.985	-	5.004	-	5.004	-
5	4.995	5.012	5.014	5.025	5.014	5.020
6	5.000	5.025	5.019	5.029	5.018	5.025
7	5.006	5.036	5.025	5.040	5.022	5.040
8	5.015	-	5.030	-	5.030	-
9	5.020	-	5.038	-	5.036	-
10	5.026	5.042	5.044	5.050	5.045	5.050
11	5.035	5.048	5.050	5.054	5.050	5.056
12	5.039	-	5.056	-	5.055	-

Thermocouple No.	<u>Series B</u>					
	Run No. 10		Run No. 11		Run No. 12	
	Liquid Side	Vapor Side	Liquid Side	Vapor Side	Liquid Side	Vapor Side
1	4.894	4.898	4.980	4.980	4.740	4.742
2	4.905	4.910	4.983	4.985	4.748	4.750
3	4.910	4.916	4.990	5.002	4.755	4.764
4	4.930	-	4.992	-	4.761	-
5	4.942	4.950	4.997	5.010	4.772	4.788
6	4.948	4.954	5.000	5.020	4.785	4.802
7	4.955	4.960	5.006	5.030	4.806	4.812
8	4.962	-	5.012	-	4.820	-
9	4.975	-	5.019	-	4.890	-
10	4.988	4.992	5.025	5.040	4.932	4.942
11	4.995	4.998	5.034	5.049	4.960	4.970
12	5.000	-	5.040	-	4.965	-

TABLE XI (continued)

Water

Series C

Thermocouple No.	Run No. 13		Run No. 14		Run No. 15	
	Liquid Side	Vapor Side	Liquid Side	Vapor Side	Liquid Side	Vapor Side
1	4.935	4.950	4.945	4.960	4.950	4.965
2	4.945	4.955	4.954	4.963	4.958	4.970
3	4.945	4.958	4.970	4.975	4.975	4.980
4	4.945	-	-	-	4.970	-
5	4.945	4.958	4.967	4.965	4.965	4.985
6	4.950	4.963	4.960	4.965	4.970	4.987
7	4.950	4.963	4.965	4.975	4.980	4.987
8	4.950	-	4.975	-	4.980	-
9	4.950	-	4.975	-	4.980	-
10	4.950	4.965	4.975	4.990	4.980	4.990
11	4.970	4.978	4.985	4.990	4.990	4.995
12	4.970	-	4.987	-	4.990	-

Thermocouple No.	Run No. 16		Run No. 17	
	Liquid Side	Vapor Side	Liquid Side	Vapor Side
1	4.937	4.940	4.940	4.950
2	4.940	4.952	4.950	4.970
3	4.955	4.965	4.968	4.975
4	4.952	-	4.965	-
5	4.945	4.965	4.960	4.975
6	4.940	4.965	4.960	4.975
7	4.950	4.968	4.965	4.977
8	4.970	-	4.977	-
9	4.980	-	4.980	-
10	4.986	5.002	4.980	4.990
11	4.995	5.014	4.983	4.995
12	5.000	-	4.985	-

TABLE XI (continued)

Series D

Thermocouple No.	Run No. 18		Run No. 19		Run No. 20	
	Liquid Side	Vapor Side	Liquid Side	Vapor Side	Liquid Side	Vapor Side
1	5.095	5.110	4.960	4.968	4.970	4.976
2	5.093	5.100	4.970	4.975	4.965	4.970
3	5.092	5.095	4.982	4.990	4.962	4.968
4	5.090	-	4.985	-	4.960	-
5	5.085	5.090	4.985	4.993	4.960	4.965
6	5.080	5.085	4.987	4.995	4.952	4.960
7	5.080	5.085	4.985	4.990	4.950	4.960
8	5.075	-	4.980	-	4.942	-
9	5.070	-	4.975	-	4.940	-
10	5.065	5.079	4.985	4.990	4.935	4.945
11	5.065	5.074	4.990	5.000	4.930	4.945
12	5.065	-	5.012	-	4.930	-

Thermocouple No.	Run No. 21		Run No. 22	
	Liquid Side	Vapor Side	Liquid Side	Vapor Side
1	4.960	4.970	4.952	4.965
2	4.965	4.967	4.950	4.960
3	4.960	4.965	4.945	4.957
4	4.960	-	4.942	-
5	4.952	4.954	4.935	4.954
6	4.950	4.952	4.930	4.950
7	4.945	4.950	4.930	4.950
8	4.940	-	4.928	-
9	4.933	-	4.925	-
10	4.930	4.943	4.923	4.938
11	4.930	4.944	4.920	4.935
12	4.925	-	4.918	-

Remark: No response from thermocouples No. 4, 8, 9, and 12 on the vapor side.

TABLE XII
TEMPERATURE DISTRIBUTION ALONG THE COIL

n-Hexane

Series A

No.	Run No. 1 $U_{\text{initial}} = 0.0188 \text{ ft/sec}$			Run No. 2 $U_{\text{initial}} = 0.0403 \text{ ft/sec}$		
	T_L -°F	T_V -°F	$(T_V - T_L)$ -°F	T_L -°F	T_V -°F	$(T_V - T_L)$ -°F
1	241.30	241.30	0.00	237.93	238.30	0.47
2	241.30	241.30	0.00	238.00	238.48	0.48
3	241.00	241.00	0.00	238.17	239.11	0.94
4	240.92	-	-	238.52	-	-
5	240.82	240.62	-0.20	238.70	239.32	0.62
6	240.62	240.62	0.00	238.89	239.48	0.59
7	240.54	240.54	0.00	239.11	239.85	0.74
8	240.35	-	-	239.30	-	-
9	240.20	-	-	239.48	-	-
10	240.05	240.05	0.00	239.58	240.77	1.19
11	240.02	240.02	0.00	239.76	240.85	1.09
12	239.76	-	-	240.06	-	-

No.	Run No. 3 $U_{\text{initial}} = 0.0685 \text{ ft/sec}$			Run No. 4 $U_{\text{initial}} = 0.0887 \text{ ft/sec}$		
	T_L -°F	T_V -°F	$(T_V - T_L)$ -°F	T_L -°F	T_V -°F	$(T_V - T_L)$ -°F
1	238.74	238.74	0.00	236.04	237.62	1.58
2	238.96	238.96	0.00	236.25	237.81	1.56
3	239.11	239.30	0.19	236.39	238.38	1.99
4	239.28	-	-	236.68	-	-
5	239.48	239.58	0.10	236.85	238.50	1.65
6	239.58	239.63	0.04	237.07	238.70	1.63
7	239.63	239.70	0.07	237.31	238.89	1.58
8	240.02	-	-	237.54	-	-
9	240.20	-	-	237.81	-	-
10	240.37	240.42	0.05	238.00	239.11	1.11
11	240.62	240.62	-	238.22	239.30	1.08
12	240.82	-	-	238.47	-	-

TABLE XII (continued)

No.	Run No. 5 $U_{\text{initial}} = 0.1450 \text{ ft/sec}$			Run No. 6 $U_{\text{initial}} = 0.1680 \text{ ft/sec}$		
	T_L - $^{\circ}\text{F}$	T_V - $^{\circ}\text{F}$	$(T_V - T_L)$ - $^{\circ}\text{F}$	T_L - $^{\circ}\text{F}$	T_V - $^{\circ}\text{F}$	$(T_V - T_L)$ - $^{\circ}\text{F}$
1	236.67	237.08	0.41	237.78	237.95	0.17
2	236.85	237.38	0.53	238.00	238.11	0.11
3	237.31	238.00	0.69	238.17	238.38	0.21
4	237.62	-	-	238.30	-	-
5	238.00	238.15	0.15	238.48	238.49	0.01
6	238.30	238.38	0.08	238.50	238.50	0.45
7	238.48	238.74	0.26	238.72	239.93	1.21
8	238.93	-	-	238.93	-	-
9	238.74	-	-	239.15	-	-
10	238.89	239.11	0.22	239.28	239.36	0.08
11	239.04	239.30	0.26	239.48	239.48	0.00
12	239.48	-	-	239.53	-	-

No.	Run No. 7 $U_{\text{initial}} = 0.1885 \text{ (approximately)}$		
	T_L - $^{\circ}\text{F}$	T_V - $^{\circ}\text{F}$	$(T_V - T_L)$ - $^{\circ}\text{F}$
1	238.40	238.46	0.06
2	238.50	238.56	0.06
3	238.74	238.93	0.19
4	238.93	-	-
5	239.30	239.93	0.63
6	239.48	240.42	0.94
7	239.70	240.85	1.15
8	240.06	-	-
9	240.24	-	-
10	240.42	241.06	0.64
11	240.82	241.29	0.47
12	240.98	-	-

TABLE XII (continued)

Series B

No.	Run No. 8 $U_{\text{initial}} = 0.0339 \text{ ft/sec}$			Run No. 9 $U_{\text{initial}} = 0.0609 \text{ ft/sec}$		
	T_L - $^{\circ}\text{F}$	T_V - $^{\circ}\text{F}$	$(T_V - T_L)$ - $^{\circ}\text{F}$	T_L - $^{\circ}\text{F}$	T_V - $^{\circ}\text{F}$	$(T_V - T_L)$ - $^{\circ}\text{F}$
1	238.89	239.34	0.45	238.96	239.11	0.15
2	239.15	239.85	0.70	239.11	239.48	0.37
3	239.32	240.32	1.00	239.85	240.05	0.20
4	239.63	-	-	239.63	-	-
5	240.02	240.42	0.40	240.02	240.24	0.22
6	240.20	240.57	0.37	240.15	240.42	0.27
7	240.42	241.00	0.58	240.30	241.00	0.70
8	240.62	-	-	240.62	-	-
9	240.90	-	-	240.85	-	-
10	241.15	241.38	0.23	241.20	241.38	0.18
11	241.38	241.52	0.14	241.38	241.59	0.21
12	241.59	-	-	241.55	-	-

No.	Run No. 10 $U_{\text{initial}} = 0.1010 \text{ ft/sec}$			Run No. 11 $U_{\text{initial}} = 0.1450 \text{ ft/sec}$		
	T_L - $^{\circ}\text{F}$	T_V - $^{\circ}\text{F}$	$(T_V - T_L)$ - $^{\circ}\text{F}$	T_L - $^{\circ}\text{F}$	T_V - $^{\circ}\text{F}$	$(T_V - T_L)$ - $^{\circ}\text{F}$
1	235.52	235.67	0.15	238.74	238.74	0.00
2	235.85	236.11	0.26	238.85	238.93	0.08
3	236.93	236.33	0.40	239.11	239.58	0.47
4	236.85	-	-	239.18	-	-
5	237.31	237.62	0.31	239.31	239.80	0.49
6	237.54	237.78	0.24	239.48	240.24	0.76
7	237.81	238.00	0.19	239.70	240.62	0.92
8	238.11	-	-	239.92	-	-
9	238.50	-	-	240.20	-	-
10	239.04	239.18	0.14	240.42	241.00	0.58
11	239.30	239.36	0.06	240.77	241.33	0.56
12	239.48	-	-	241.00	-	-

TABLE XII (continued)

Run No. 12
 $U_{\text{initial}} = 0.1730 \text{ ft/sec}$

No.	T_L - $^{\circ}\text{F}$	T_V - $^{\circ}\text{F}$	$(T_V - T_L)$ - $^{\circ}\text{F}$
1	230.35	230.42	0.07
2	230.50	230.81	0.31
3	230.00	230.58	0.58
4	230.64	-	-
5	230.89	231.50	0.61
6	231.39	232.04	0.65
7	232.19	232.42	0.23
8	232.73	-	-
9	236.38	-	-
10	237.08	237.31	0.23
11	238.00	238.38	0.38
12	238.17	-	-

Water

Series C

No.	Run No. 13 $U_{\text{initial}} = 0.1030 \text{ ft/sec}$			Run No. 14 $U_{\text{initial}} = 0.1514 \text{ ft/sec}$		
	T_L - $^{\circ}\text{F}$	T_V - $^{\circ}\text{F}$	$(T_V - T_L)$ - $^{\circ}\text{F}$	T_L - $^{\circ}\text{F}$	T_V - $^{\circ}\text{F}$	$(T_V - T_L)$ - $^{\circ}\text{F}$
1	237.04	237.62	0.58	237.42	238.00	0.58
2	237.42	237.81	0.39	237.78	238.11	0.33
3	237.42	237.92	0.50	238.37	238.50	0.13
4	237.42	-	-	238.27	-	-
5	237.42	237.92	0.50	238.00	238.19	0.19
6	237.62	238.11	0.49	238.00	238.19	0.19
7	237.62	238.11	0.49	238.19	238.50	0.31
8	237.62	-	-	238.50	-	-
9	237.62	-	-	238.50	-	-
10	237.62	238.19	0.57	238.93	239.11	0.61
11	238.37	238.67	0.30	238.99	239.11	0.12
12	238.37	-	-			

TABLE XII (continued)

No.	Run No. 15 $U_{\text{initial}} = 0.1890 \text{ ft/sec}$			Run No. 16 $U_{\text{initial}} = 0.2340 \text{ ft/sec}$		
	T_L - $^{\circ}\text{F}$	T_V - $^{\circ}\text{F}$	$(T_V - T_L)$ - $^{\circ}\text{F}$	T_L - $^{\circ}\text{F}$	T_V - $^{\circ}\text{F}$	$(T_V - T_L)$ - $^{\circ}\text{F}$
1	237.62	238.19	0.57	237.11	237.23	0.12
2	237.92	238.37	0.45	237.23	237.69	0.46
3	238.50	238.74	0.24	237.81	238.19	0.38
4	238.37	-	-	237.69	-	-
5	238.19	238.93	0.74	237.42	238.19	0.77
6	238.37	238.99	0.62	237.23	238.19	0.96
7	238.74	238.99	0.25	237.62	238.19	0.57
8	238.74	-	-	238.32	-	-
9	238.74	-	-	238.74	-	-
10	238.74	239.11	0.37	238.96	239.76	0.80
11	239.11	239.30	0.19	239.30	240.00	0.70
12	239.11	-	-	239.48	-	-

No.	Run No. 17 $U_{\text{initial}} = 0.4040 \text{ ft/sec}$		
	T_L - $^{\circ}\text{F}$	T_V - $^{\circ}\text{F}$	$(T_V - T_L)$ - $^{\circ}\text{F}$
1	237.23	237.62	0.39
2	237.62	238.37	0.75
3	238.30	238.50	0.20
4	238.19	-	-
5	238.00	238.50	0.50
6	238.00	238.50	0.50
7	238.19	238.63	0.44
8	238.63	-	-
9	238.74	-	-
10	238.74	239.11	0.37
11	238.85	239.30	0.45
12	238.93	-	-

TABLE XII (continued)

Series D

No.	Run No. 18 $U_{\text{initial}} = 0.0153 \text{ ft/sec}$			Run No. 19 $U_{\text{initial}} = 0.0216 \text{ ft/sec}$		
	T_L -°F	T_V -°F	$(T_V - T_L)$ -°F	T_L -°F	T_V -°F	$(T_V - T_L)$ -°F
1	243.04	243.62	0.58	238.00	238.30	0.30
2	242.96	243.23	0.27	238.37	238.50	0.13
3	242.93	243.04	0.11	238.82	239.11	0.29
4	242.85	-	-	238.93	-	-
5	242.67	242.85	0.18	238.93	239.22	0.29
6	242.48	242.67	0.19	238.99	239.30	0.31
7	242.48	242.67	0.19	238.93	239.11	0.18
8	242.30	-	-	238.74	-	-
9	242.11	-	-	238.50	-	-
10	241.93	242.44	0.51	238.95	239.11	0.16
11	241.93	242.26	0.33	239.11	239.48	0.37
12	241.93	-	-	239.92	-	-

No.	Run No. 20 $U_{\text{initial}} = 0.0303 \text{ ft/sec}$			Run No. 21 $U_{\text{initial}} = 0.0431 \text{ ft/sec}$		
	T_L -°F	T_V -°F	$(T_V - T_L)$ -°F	T_L -°F	T_V -°F	$(T_V - T_L)$ -°F
1	238.37	238.59	0.22	238.00	238.37	0.37
2	238.19	238.37	0.18	238.19	238.27	0.08
3	238.11	238.30	0.19	238.00	238.19	0.19
4	238.00	-	-	238.00	-	-
5	238.00	238.19	0.19	237.69	237.77	0.08
6	237.69	238.00	0.31	237.62	237.69	0.07
7	237.62	238.00	0.38	237.42	237.62	0.20
8	237.31	-	-	237.23	-	-
9	237.23	-	-	236.96	-	-
10	237.04	237.42	0.38	236.85	237.33	0.48
11	236.85	237.08	0.23	236.85	237.34	0.49
12	236.85	-	-	236.67	-	-

TABLE XII (continued)

No.	Run No. 22		
	T_L -°F	T_V -°F	$(T_V - T_L)$ -°F
1	237.69	238.19	0.50
2	237.62	238.00	0.38
3	237.42	237.89	0.47
4	237.31	-	-
5	237.04	237.77	0.73
6	236.85	237.62	0.77
7	236.85	237.62	0.77
8	236.78	-	-
9	236.67	-	-
10	236.59	237.15	0.56
11	236.48	237.04	0.56
12	236.41	-	-

Remark: No response from thermocouples No. 4, 8, 9 and 12 on the vapor side.

APPENDIX B

SAMPLE CALCULATIONS

SAMPLE CALCULATIONS

Estimation of Boiling Heat Flux

Run No. 6

Estimation of A_{PH} . Since the wall is at about 240° F, subcooled boiling will occur. The following calculations are based upon Dittus Bolter Correlation and will only estimate A_{PH} .

Basis for calculations. The heat transfer area is taken as the inside area of the tubing. Over-all temperature difference is used. The copper tubing wall resistance to heat transfer is negligible and the coefficient of steam condensation outside the wall is very big compared to any other coefficient.

$T_{in} = 105^\circ$ F	$\rho = 39.3$ lb _m /cu ft
$T_{out} = 156^\circ$ F	$\mu = 1.68 \times 10^{-4}$ lb _m /ft sec
$T_{av} = 130.5^\circ$ F	$k = 0.08$ BTU/hr sq ft $^\circ$ F/ft
$D = 0.044$ ft	$s = 0.1382$ sq ft/ft
$U_o = 0.168$ ft/sec (or 605 ft/hr)	

$$Nu_{am} = \frac{h_{am} D}{k} = 1.62 (Pe)^{1/3} \frac{D}{L} \left(\frac{\mu_b}{\mu_w} \right)^{0.14} \quad (1)$$

$$Re = \frac{DU\rho}{\mu} = \frac{(0.044)(0.168)(39.3)}{1.68 \times 10^{-4}} = 1730$$

$$Pe = \frac{DU\rho C_p}{k} = \frac{(0.044)(605)(39.3)(0.680)}{0.08} = 8900$$

$$Pe^{1/3} = 20.7$$

$$(\mu_b/\mu_w)^{0.14} = (0.25/0.24)^{0.14} = 1.0025$$

$$(D/0.08)h_{am} = (1.62)(20.7)(1.0025)(D/L)^{1/3}$$

$$h_{am} = (2.68/D)(D/L)^{1/3} \quad (2)$$

$$q_{PH} = 1310 = (h_{am})(\pi)(D)(L)(\Delta T_{am}) \quad (3)$$

$$\Delta T_{am} = \frac{(240 - 156) + (240 - 105)}{2} = 110^\circ \text{ F}$$

from equation (3)

$$h_{am} = \frac{1310}{(110)(\pi)(D)(L)} = \frac{3.79}{DL} \quad (4)$$

equating equations (2) and (4)

$$(2.68/D)(D/L)^{1/3} = 3.79/(D)(L) \quad (5)$$

$$(L)^{2/3}(D)^{1/3} = 1.47 \quad (6)$$

$$(L)^{2/3} = (1.47)(0.044)^{-1/3} = 4.15 \quad (7)$$

$$L = 8.45 \text{ ft}$$

$$A_{PH} = (L)(S) = (8.45)(0.1382) = 1.17 \text{ sq ft}$$

Estimation of A_{SH} .

For n-hexane vapor:

$$k = 0.0109 \text{ BTU}/(\text{hr})(\text{sq ft})(^\circ\text{F})/\text{ft}$$

$$\text{Re} = 55,600 \quad T_{in} = 156^\circ \text{ F}$$

$$\text{Pr} = 0.925 \quad T_{out} = 229^\circ \text{ F}$$

$$\text{Nu} = 0.023(\text{Re})^{0.8}(\text{Pr})^{0.4} \quad (8)$$

$$\text{Nu} = hD/k = (0.023)(55,600)^{0.8}(0.925)^{0.4} \quad (9)$$

From equation (9)

$$h = \frac{(0.023)(55,600)^{0.8}(0.925)^{0.4}(0.0109)}{0.044} = 34.3 \text{ BTU}/(\text{hr})(\text{sq ft})(^\circ\text{F})$$

$$q_{SH} = 1275 \text{ BTU/hr} = A_{SH}h(\Delta T)_{LM}$$

$$(\Delta T)_{LM} = \frac{(240 - 156) - (240 - 229)}{\ln \frac{240 - 156}{240 - 229}} = 36.2^\circ \text{ F}$$

$$A_{SH} = \frac{q_{SH}}{(h)(\Delta T)_{LM}} = \frac{1275}{(34.4)(36.2)} = 1.02 \text{ sq ft}$$

Estimation of $(q/A)_B$.

$$\text{Total inside area: } A_{\text{total}} = 3.3 \text{ sq ft}$$

$$A_B = 3.3 - (1.17 + 1.02) = 1.11 \text{ sq ft}$$

$$q_B = 5440 \text{ BTU/hr}$$

and,

$$(q/A)_B = 5440/1.11 = 4900 \text{ BTU/(sq ft)(hr)}$$

Dimensionless Radial Acceleration

For n-hexane, run no. 6 and vapor fraction of 50%.

$$U_o = 0.168 \text{ ft/sec}$$

$$R = 0.297 \text{ ft}$$

$$\frac{\rho_L}{\rho_V} = \frac{40.8}{0.191} = 214$$

$$g = 32.17 \text{ ft/sec}^2$$

$$x = 0.5$$

$$\frac{a_r}{g} = \frac{(214)(0.168)(0.5)^2}{(0.297)(32.17)} = 33.9$$

For water, run no. 22 and vapor fraction of 50%.

$$U_o = 0.0525 \text{ ft/sec}$$

$$x = 0.5$$

$$\frac{\rho_L}{\rho_V} = \frac{V_V}{V_L} = \frac{26.8}{0.01672} = 1600$$

$$R = 0.297 \text{ ft}$$

$$\frac{a_r}{g} = \frac{(1600)(0.0525)(0.5)^2}{(0.297)(32.17)} = 185.5$$

APPENDIX C

THERMOCOUPLE CALIBRATION PROCEDURE

THERMOCOUPLE CALIBRATION PROCEDURE

One thermocouple, designated as "reference thermocouple" was calibrated at two fixed temperatures. This "reference thermocouple" was inserted into the evaporator and the potentiometer readings of the 24 thermocouples attached to the coil wall were corrected according to the "reference thermocouple" for two constant temperatures (see Table XIII and Table XIV).

The two temperatures mentioned above were obtained by: (1) evaporator at room temperature, (no steam was used) and (2) evaporated heated by steam at 240° F to steady state (no liquid introduced).

Calibration of the Reference Thermocouple

The two constant temperatures were the temperature of boiling water at absolute pressure of 739.5 mm Hg and of water at 77.95° F. The calibration data are given in the table below:

TABLE XIII
CALIBRATION OF THE REFERENCE THERMOCOUPLE

Potentiometer Reading-mv	Temperature °F	Reference Thermocouple Temperature °F
4.242	210.65	210.65
1.012	77.95	78.00

Then the thermocouple calibration table can be used. The temperature recording procedure is as follows:

- (a) record potentiometer reading
- (b) correct this reading according to the "reference thermocouple"
- (c) obtain the temperature in °F.

Reference thermocouple reading inside the evaporator.

High Temperature:	4.992 mv
(Evaporator at steam temperature)	5.000 mv
	average: 4.996 mv
Low temperature:	0.868 mv
(Evaporator at room temperature)	0.888 mv
	average: 0.878 mv

TABLE XIV
THERMOCOUPLE READING CORRECTION
Low Temperature

Point No.	<u>Liquid Side</u>			<u>Vapor Side</u>		
	Potent. Reading mv	Ave. Reading mv	Correction mv	Potent. Reading mv	Ave. Reading mv	Correction mv
1	0.879			0.882		
	0.899	0.889	-0.011	0.899	0.891	-0.013
2	0.880			0.882		
	0.899	0.890	-0.012	0.899	0.891	-0.013
3	0.880			0.882		
	0.899	0.890	-0.012	0.899	0.891	-0.013
4	0.880			0.882		
	0.899	0.890	-0.012	0.899	0.891	-0.013
5	0.880			0.882		
	0.899	0.890	-0.012	0.899	0.891	-0.013
6	0.877			0.882		
	0.899	0.888	-0.010	0.899	0.891	-0.013
7	0.877			0.880		
	0.899	0.888	-0.010	0.902	0.891	-0.013
8	0.877			0.880		
	0.899	0.888	-0.010	0.902	0.902	-0.013
9	0.877			*		
	0.899	0.888	-0.010			
10	0.879			0.880		
	0.899	0.889	-0.011	0.900	0.885	-0.007
11	0.879			0.880		
	0.899	0.889	-0.011	0.900	0.885	-0.007
12	0.879			*		
	0.895	0.887	-0.009			*Out of order

TABLE XV
THERMOCOUPLE READING CORRECTION

High Temperature

Point No.	<u>Liquid Side</u>			<u>Vapor Side</u>		
	Potent. Reading mv	Ave. Reading mv	Correction mv	Potent. Reading mv	Ave. Reading mv	Correction mv
1	4.993	4.996	0.0	4.975	4.982	+0.014
	4.999			4.988		
2	4.993	4.996	0.0	4.975	4.982	+0.014
	4.999			4.988		
3	4.994	4.997	-0.001	4.977	4.984	+0.012
	4.999			4.990		
4	4.995	4.998	-0.002	*		
	5.000					
5	4.995	4.999	-0.003	4.978	4.984	+0.012
	5.002			4.990		
6	4.996	4.999	-0.003	4.977	4.986	+0.010
	5.002			4.994		
7	4.996	5.001	-0.005	4.983	4.989	+0.007
	5.005			4.994		
8	4.987	5.001	-0.005	4.985		
	5.005			*		
9	4.997	5.002	-0.006	*		
	5.007					
10	5.000	5.004	-0.008	4.983	4.989	+0.007
	5.007			4.994		
11	5.000	5.004	-0.008	4.985	4.990	+0.006
	5.007			4.995		
12	5.000	6.006	-0.010	*		*Out of Order
	5.012					

APPENDIX D

ROTAMETER AND ORIFICE CALIBRATION

TABLE XVI
COOLING WATER ORIFICE FLOW METER CALIBRATION

Orifice Manometer Reading inch Hg	Time sec	Water Weight lbs	Cooling Water Flow Rate lbs/min
1.10	71.2	14.06	11.85
2.35	46.5	13.65	17.61
3.15	32.2	11.01	20.55
4.80	34.2	13.80	24.20
5.35	33.7	15.06	26.80
5.75	33.3	15.54	28.00
8.00	23.2	12.61	32.60
9.60	26.7	16.02	36.00
11.00	24.6	15.64	38.15
12.7	20.6	15.16	44.2

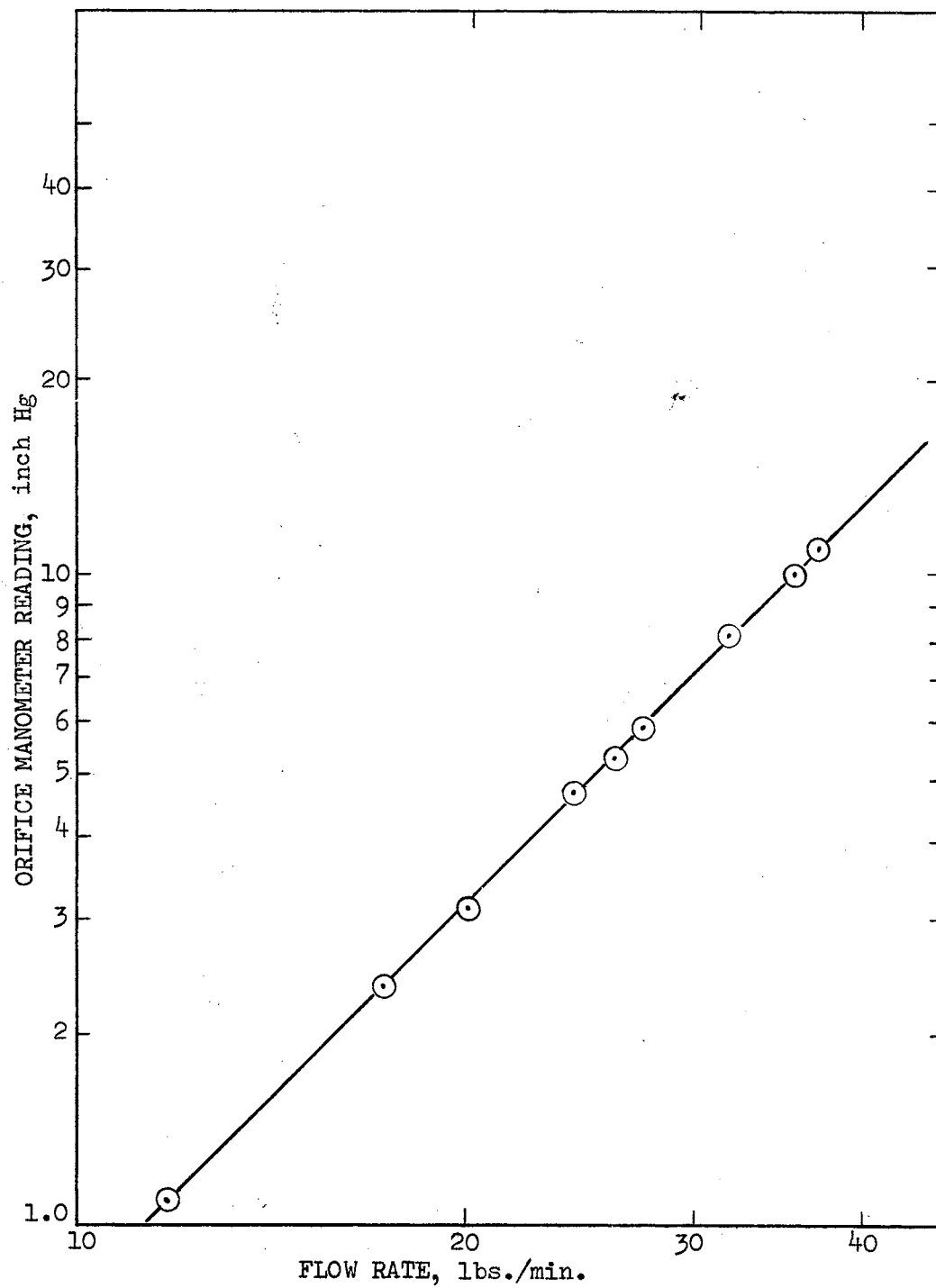


Figure 24. Cooling Water Orifice Calibration Curve

TABLE XVII
ROTAMETER CALIBRATION FOR N-HEXANE

Black Float Scale Division	White Float Scale Division	Time min	Volume liter	Flow Rate liter/min
1.9	0.9	4.292	0.250	0.058
4.4	2.3	2.142	0.440	0.205
5.0	2.7	2.150	0.500	0.233
6.6	3.5	2.117	0.675	0.319
8.3	4.4	1.192	0.500	0.419
10	5.3	1.183	0.630	0.533
12.6	6.8	1.170	0.808	0.691

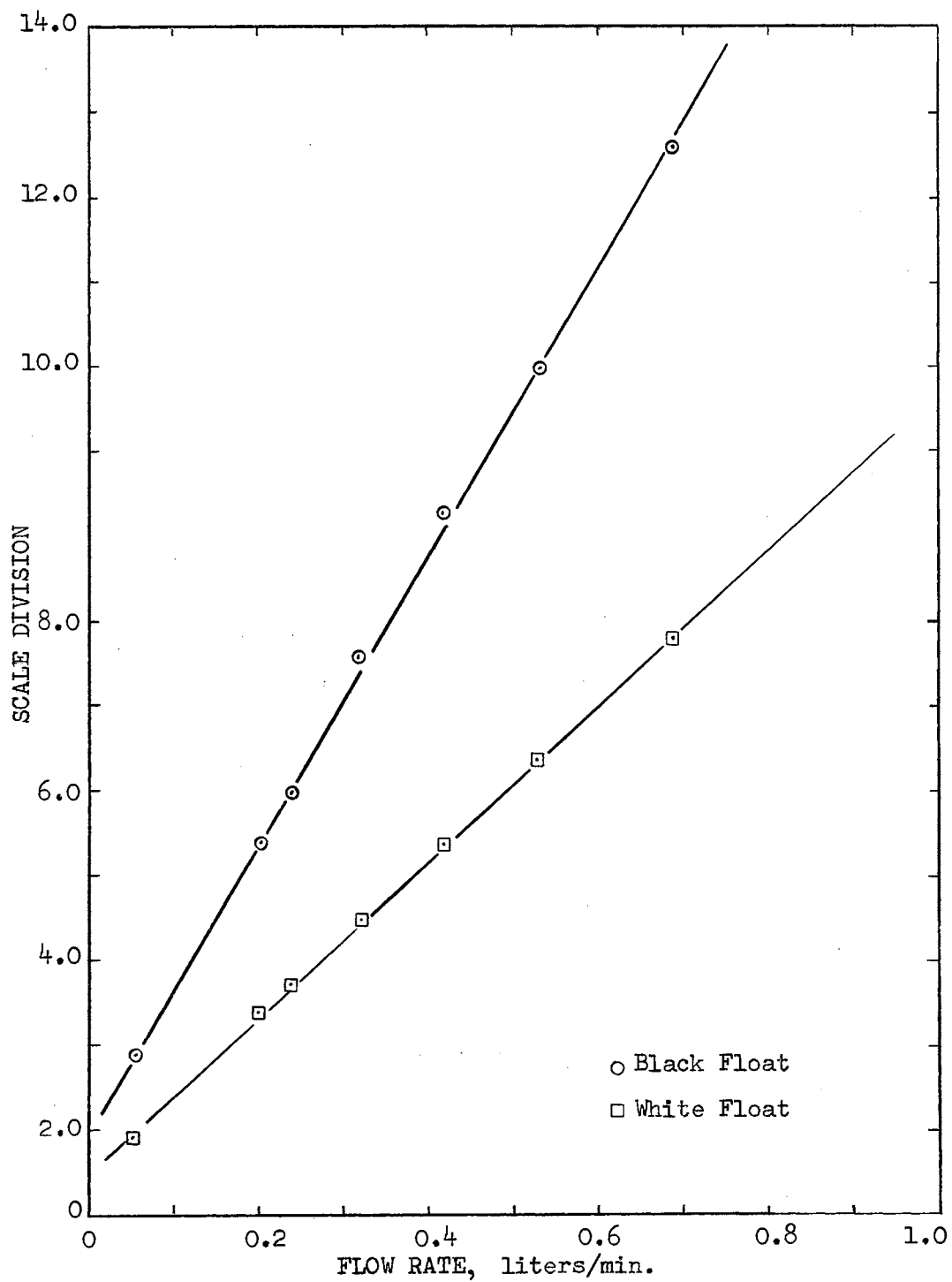


Figure 25. Rotameter Calibration Curve for n-Hexane

TABLE XVIII
ROTAMETER CALIBRATION FOR WATER

Black Float Scale Division	White Float Scale Division	Time min	Volume liter	Flow Rate liter/min
2.0	1.1	9	0.290	0.032
4.0	2.0	10	1.105	0.111
5.0	2.4	3	0.418	0.139
6.0	2.9	10	1.755	0.176
8.0	3.9	8	2.035	0.254
9.9	4.9	3	1.010	0.337
12.0	6.0	3	1.290	0.430
13.9	6.9	4	2.080	0.520
14.8	7.3	2	1.133	0.565
-	11.0	2.5	2.141	0.856

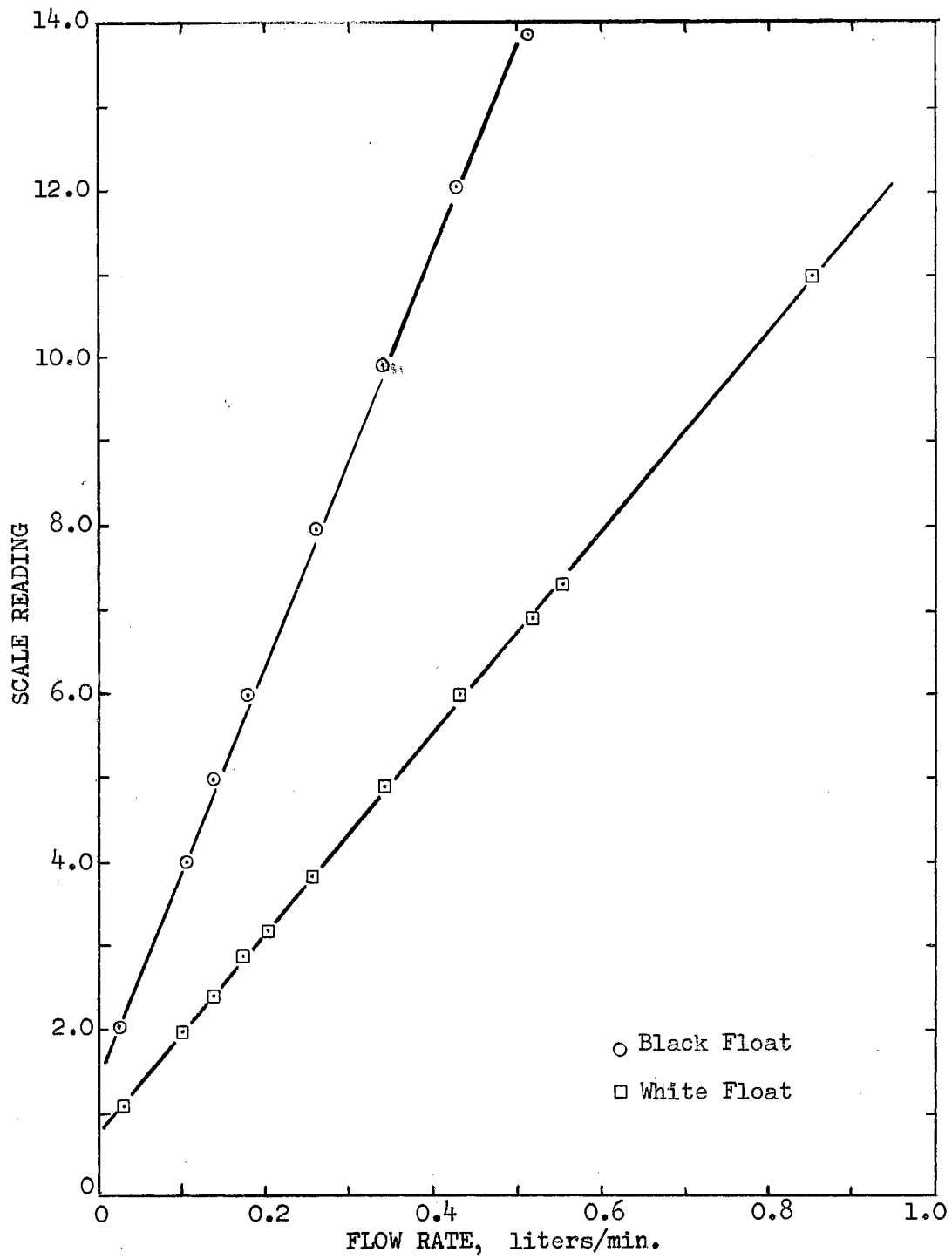


Figure 26. Rotameter Calibration Curve for Water

NOMENCLATURE

- a_r - radial acceleration, ft/sec²
- A - area, sq ft
- C_1, C^o - constants
- D - coil tubing diameter, ft
- g - gravitational acceleration, ft/sec²
- g_c - conversion factor, 32.17 (lb_m)(ft)/(lb_f)(sec²)
- G - mass flow rate, lb_m/hr
- h - heat transfer coefficient, BTU/(hr)(sq ft)(°F)
- k - thermal conductivity, BTU/(hr)(sq ft)(°F)/ft
- L - coil length, ft
- q - rate of heat transfer, BTU/hr
- P - pressure, lb_f/sq in
- S - tubing cross-section area, sq ft
- T - temperature, °F
- U - velocity, ft/hr
- v - specific volume, cu ft/lb_m
- Greek
- α - angle, degree
- ρ - density, lb_m/cu ft
- μ - viscosity, lb_m/ft sec
- ΔP - pressure difference, lb_m/sq in
- ΔT - temperature difference, °F

Subscripts

- am - arithmetic mean
- B - boiling
- b - bubble or bulk
- L - liquid
- PH - preheating
- SH - superheating
- o - initial value
- r - radial direction
- v - vapor